

# ÉCOLE POLYTECHNIQUE

MEC 596 - Research Internship

*CNRS@CREATE, DesCartes Program, Singapore*

---

## Climate change impact on renewable energy potential in Southeast Asia

---

**Lélia Choukroun-Vinh**

2023/2024 - P3



INSTITUT  
POLYTECHNIQUE  
DE PARIS



---

Supervisors: Blaise Genest & Benoit Delinchant (CNRS@CREATE, Singapore)

Coordinator: Alexis Tantet (Laboratoire de Météorologie Dynamique, École Polytechnique)



## **Abstract**

This report explores the impact of climate change on renewable energy potential in Southeast Asia, with a particular focus on hydropower generation within the Mekong River Basin. The primary objective is to identify critical features for predicting river discharge based on rainfall data, laying the groundwork for developing more complex predictive models. Using a dataset from the Mekong River Commission, spanning 2007 to 2024, this study employs statistical techniques such as time series decomposition, autocorrelation, and partial autocorrelation analyses to identify patterns and trends.

Initial findings indicate significant seasonal and lagged correlations between rainfall and river discharge, suggesting that climatic variables play a crucial role in hydropower generation. Various machine learning models, including linear regressions and decision trees, were trained and evaluated. The performance metrics of these models provide valuable insights into the predictive capabilities of different feature sets.

The research highlights the importance of integrating high-resolution climatic and hydrological data to improve the accuracy of renewable energy forecasts. While this study represents an early stage in understanding the complex interactions between climate change and renewable energy production, it offers a foundational framework for more advanced modeling efforts. The results will inform sustainable energy planning and help address the challenges posed by climate variability and extreme weather events in the region.

## Acknowledgments

I want to express my deepest gratitude to my supervisors, Benoit Delinchant and Blaise Genest, for their unwavering support, guidance, and encouragement throughout this research internship. Their expertise and insights have been invaluable to this project and my first academic research experience.

I also thank the whole lab, CNRS@CREATE, for making this experience possible and for the warm welcome upon my arrival in Singapore.

Then, thank you to Alexis Tantet for coordinating this internship and checking in to ensure everything was going nicely.

Finally, I am grateful to my fellow Polytechnique students in Singapore for sharing this incredible adventure with me, especially my friend, colleague, and roommate, Benjamin Blois.

# Contents

<b>List of Tables</b> . . . . .	<b>5</b>
<b>List of Figures</b> . . . . .	<b>6</b>
<b>Glossary</b> . . . . .	<b>7</b>
<b>1 Introduction</b> . . . . .	<b>8</b>
<b>2 Background</b> . . . . .	<b>9</b>
2.1 Hydropower . . . . .	9
2.1.1 Hydrological Variability . . . . .	10
2.1.2 Temperature Changes and Evaporation Rates . . . . .	12
2.1.3 Sedimentation and Reservoir Siltation . . . . .	13
2.1.4 Economic Impact . . . . .	13
2.2 Solar Power . . . . .	14
2.2.1 Temperature Variations . . . . .	14
2.2.2 Solar Irradiance and Weather Extremes . . . . .	15
2.2.3 Sea-Level Rise and Coastal Installations . . . . .	17
2.2.4 Economic Viability . . . . .	17
2.2.5 Technological Advancements and Infrastructure Development . . . . .	17
2.3 Wind Power . . . . .	18
2.3.1 Wind Patterns and Speed Changes . . . . .	18
2.3.2 Extreme Weather Events . . . . .	18
2.3.3 Sea-Level Rise and Coastal Erosion . . . . .	19
2.3.4 Wind Power Potential Projections . . . . .	19
2.3.5 Economic Viability . . . . .	20
2.4 Knowledge Gaps and Research Needs . . . . .	21
<b>3 General Approach and Methodology</b> . . . . .	<b>23</b>
3.1 Research Project Orientation . . . . .	23
3.2 Methods and Materials . . . . .	23
<b>4 Results and Discussion</b> . . . . .	<b>26</b>
4.1 General statistics and analysis of monthly and weekly data . . . . .	26
4.1.1 Average monthly data analysis . . . . .	26
4.1.2 Average weekly data analysis . . . . .	27
4.2 Discharge forecasting models . . . . .	32
4.2.1 Models learning on original data . . . . .	32
4.2.2 Time Series Decomposition (TSD) Approach . . . . .	36
4.2.3 Additional studies . . . . .	40
<b>5 Code and datasets availability</b> . . . . .	<b>44</b>

<b>6 Conclusions . . . . .</b>	<b>45</b>
<b>References . . . . .</b>	<b>46</b>

## List of Tables

1	Feature Sets for Linear Regression models . . . . .	32
2	Performance metrics of Linear Regression models . . . . .	33
3	Performance metrics of monthly Linear Regression models . . . . .	34
4	Feature Sets for Decision Tree models . . . . .	34
5	Performance metrics of Decision Tree models . . . . .	35
6	Performance metrics of Random Forest and XGBoost models trained on Sets 1 & 6 . . . . .	35
7	Performance metrics of Trends Linear Regressions . . . . .	38
8	Performance metrics of the superposition of projected trends with actual seasonal data . . . . .	39
9	Quantile Regression (quantile=0.25) Metrics for Stung Treng and Chiang Khan . . . . .	42
10	Evaluation Metrics for Kratie, Stung Treng, and Chiang Khan Forecasts . . . . .	43

## List of Figures

1	Lancang-Mekong River Basin map and regional hydropower projects . . . . .	9
2	The effect of climate change on global hydropower generation, based on observed trends and near-future projections. The effects are indicated by two levels of symbols: high and low. Generally, if a climate change effect is discussed in more than 50% of the review papers for the region, a "high" symbol is adopted. [2] . . . . .	10
3	Projected changes in streamflow over (a) the Lancang-Mekong River Basin (LMRB), (b) the Lancang River Basin (LRB), and (c) the Mekong River Basin (MRB) [1] . . . . .	12
4	Projections for hydropower in Southeast Asia . . . . .	13
5	Climate change impact on hydropower (the importance of a phenomenon is related to the width of its arrow and box) . . . . .	14
6	Solar power capacities repartition in 2037 over continental Southeast Asia [7]	16
7	Percent variation estimate in hydropower production potential caused by climate change [8] . . . . .	20
8	Combined relative effect of climate impacts on cumulative primary energy supply for each iMaGE model region. China+ includes Taiwan. [20] . . . . .	22
9	Prediction methodology using TSD . . . . .	25
10	Average monthly flowrate and rainfall over 2007-2024 in Stung Treng . . . . .	26
11	Weekly discharge data over 2007-2024 in Stung Treng . . . . .	27
12	TSD of weekly minimum (a), maximum (b), average flowrates(c), and total rainfall (d) for Stung Treng data over 2007-2024 . . . . .	28
13	Autocorrelation Function (ACF) and Partial Autocorrelation Function (PACF) of weekly minimum (a), maximum (b), average flowrates(c), and total rainfall (d) for Stung Treng data over 2007-2024 . . . . .	29
14	Correlation heatmaps for Stung Treng weekly data (avg = average, min = minimum, max = maximum) . . . . .	30
15	Weekly average flowrate-total rainfall cross-correlation for Stung Treng data over 2007-2024 . . . . .	31
16	Random Forest model for Set 1 . . . . .	36
17	Decomposition of Stung Treng flowrate data over 2007-2024 . . . . .	37
18	Trends for rainfall, flowrate, and weekly rainfall data in Stung Treng data over 2007-2024 . . . . .	37
19	Trend features correlation heatmap . . . . .	38
20	Linear regressions based on the four datasets prepared using TSD . . . . .	39
21	Stung Treng dataset correlation heatmap (elec = annual hydropower generation in Cambodia, rice = annual rice production in Cambodia, rainfall_5weeks = total rainfall over the past 5 weeks) . . . . .	41
22	Chiang Khan and Stung Treng combined dataset correlation heatmap . . . . .	42
23	Plots of Stung Treng and Chiang Khan 25th quantile regressions . . . . .	43
24	Regressors comparison for Stung Treng, Chiang Khan and Kratie . . . . .	44

---

## Acronyms

**ACF** Autocorrelation Function. 6, 29

**ASEAN** Association of Southeast Asian Nations. 10

**CREATE** Campus for Research Excellence and Technological Enterprise. 8

**ENSO** El Niño-Southern Oscillation. 18, 21

**GCM** Global Climate Model. 11

**GDP** Gross Domestic Product. 24, 26, 32, 33, 38, 41

**HMA** High Mountain Asia. 11

**IMF** International Monetary Fund. 24, 40

**IPCC** Intergovernmental Panel on Climate Change. 10, 18

**LMR** Lancang-Mekong River. 9

**LMRB** Lancang-Mekong River Basin. 6, 11, 12

**LRB** Lancang River Basin. 6, 9, 11, 12

**MRB** Mekong River Basin. 6, 9–12, 24

**MRC** Mekong River Commission. 24

**MSE** Mean Squared Error. 33–35, 38, 39, 43

**PACF** Partial Autocorrelation Function. 6, 29

**PV** photovoltaic. 14, 15, 17

**RCP** Representative Concentration Pathways. 11, 21

**STL** Seasonal and Trend decomposition using Loess (locally weighted scatterplot smoothing). 36–39

**TSD** Time Series Decomposition. 3, 6, 24, 25, 28, 30, 31, 36–39

# 1 Introduction

The increasing global demand for energy and the urgent need to reduce carbon emissions have driven a significant shift towards renewable energy sources. With its abundant natural resources, Southeast Asia has a vast potential for renewable energy production, particularly solar, wind, and hydroelectric power. However, the region also faces unique challenges related to climate variability, geographic diversity, and economic disparities, which can impact the reliability and efficiency of renewable energy production.

This long-term research project focuses on predicting renewable energy production in Southeast Asia. It aims to enhance the accuracy and reliability of these predictions to support sustainable energy planning and management. By leveraging climate forecasts, data science techniques, and mechanical principles, the project seeks to address the critical need for accurate power generation forecasting models that can accommodate the region's dynamic environmental conditions.

Throughout this internship, various data-driven approaches, including machine learning algorithms and statistical methods, preceded by a thorough literature review to identify knowledge gaps, were explored to develop predictive models for renewable energy output. The research emphasizes the integration of climatic, geographical, and historical generation data to improve the robustness of these models. Indeed, this groundwork is necessary as the work presented in this report represents the early stages of the project. Specifically, we focus on a specific location on the Mekong River to understand critical features and forecast the local minimum hydropower generation that could be obtained.

This project, while being an academic research endeavor, was commissioned by Singapore as part of their efforts to go green and meet a growing energy demand through the import of renewable energy. Consequently, governmental agencies require accurate long-term generation forecasts and risk assessments to ensure a minimum renewable power generation at all times. The Campus for Research Excellence and Technological Enterprise (CREATE) initiative in Singapore provided a collaborative research environment that facilitated this study. The project represents the initial phase of a sustained effort, with ongoing work to continue after the conclusion of this internship.

## 2 Background

Southeast Asia benefits from abundant renewable energy resources, including significant hydropower, solar, and wind energy potential. These resources are crucial for the region's sustainable development and efforts to reduce greenhouse gas emissions. However, climate change poses substantial risks to the sustainability and efficiency of these renewable energy sources. This comprehensive literature review delves into the impacts of climate change on hydropower, solar, and wind energy in Southeast Asia. It looks into detailed insights into future production potentials, geographical variations, and necessary adaptation strategies while identifying critical knowledge gaps that must be addressed.

### 2.1 Hydropower

Hydropower is a cornerstone of Southeast Asia's energy landscape, especially in Laos, Vietnam, and Cambodia. The Lancang-Mekong River (LMR) plays a crucial role in hydropower production. Originating from the Qinghai-Tibet Plateau in China, the LMR flows through six nations before draining into the South China Sea. It spans 4880 km, making it the longest river in Southeast Asia, the seventh longest in Asia, and the twelfth longest in the world. The river basin covers 795,000 km<sup>2</sup>, making it the tenth largest river basin globally. Over 70 million people rely on the LMR for water supply, food production, and transportation. The upper portion, known as the LRB, flows through China, while the lower portion, the MRB, flows through Myanmar, Laos, Thailand, Cambodia, and Vietnam [1] (see Figure 1).

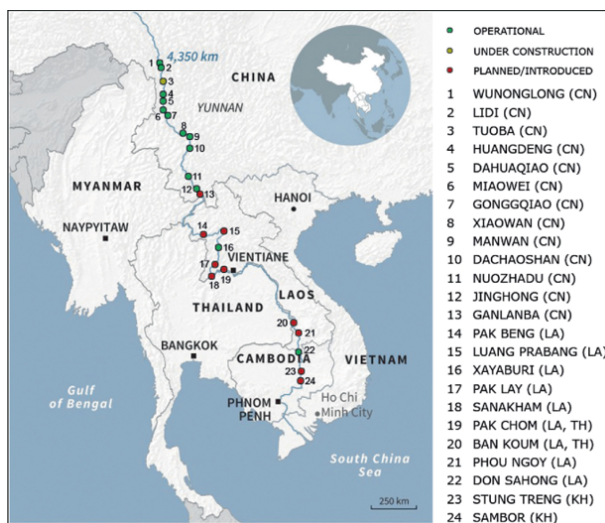


Figure 1: Lancang-Mekong River Basin map and regional hydropower projects

Despite its importance, the viability of hydropower in this region is increasingly jeopardized by climate change. The impacts of climate change, including hydrological variability, rising temperatures, evaporation rates, sedimentation, and economic repercussions, present significant challenges to the sustainability and efficiency of hydropower systems at multiple scales, as shown in Figure 2.

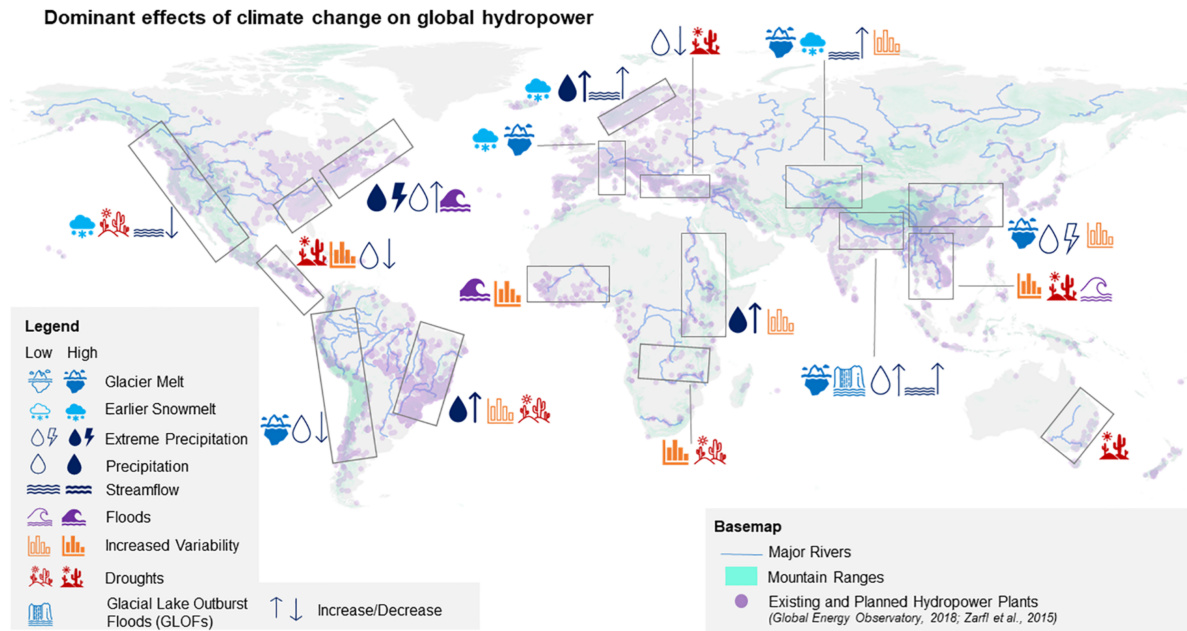


Figure 2: The effect of climate change on global hydropower generation, based on observed trends and near-future projections. The effects are indicated by two levels of symbols: high and low. Generally, if a climate change effect is discussed in more than 50% of the review papers for the region, a "high" symbol is adopted. [2]

### 2.1.1 Hydrological Variability

Hydrological variability driven by climate change substantially threatens hydropower in Southeast Asia. The Intergovernmental Panel on Climate Change (IPCC) projects that annual mean precipitation in Southeast Asia could increase by up to 7% by 2050 under high-emission scenarios [3]. Increased frequency and severity of droughts can significantly reduce river flows, decreasing water availability for hydropower generation. Severe droughts in the Association of Southeast Asian Nations (ASEAN) region have historically resulted in significant reductions in hydropower capacity, with some plants operating at less than 50% capacity during extreme drought periods [1, 2, 4]. Conversely, excessive rainfall and flooding can disrupt hydropower operations by causing dam overflow and structural damage. The Mekong River Basin experienced extreme flooding between 2010 and 2020, resulting in damages exceeding \$5 billion and significant disruptions to hydropower production [1].

RCP6.0 envisions emissions peaking around 2080, with stabilization of radiative forcing at  $6.0 \text{ W/m}^2$  by 2100 through advanced emission reduction technologies, leading to a potential global temperature increase of 3–4°C. In contrast, RCP8.5, considered a worst-case scenario, assumes a continuous rise in emissions throughout the 21st century. Although now seen as improbable, RCP8.5 remains relevant for projecting potential emissions under current policies up to mid-century. Wang et al. (2024) [5] conducted a comprehensive study on the historical and projected future runoff over the MRB under various climate scenarios. Despite the establishment of dams and reservoirs, annual runoff in the MRB has not changed significantly over the past five decades. However, future projections under

various Representative Concentration Pathways (RCP) indicate significant increases in runoff, especially in the middle and lower reaches of the basin. Under RCP6.0, runoff could increase by up to 13%, particularly during the rainy season, exacerbating flood risks, while reduced water availability during the dry season could worsen water scarcity. In the mid-term future (up to 2050), accelerated glacial melt due to rising temperatures is expected to increase river flow and runoff during the wet season, further heightening flood risks and challenging hydropower infrastructure management. In the long term (beyond 2050 to 2100), prolonged droughts are anticipated under high-emission scenarios like RCP8.5, leading to reduced precipitation, increased evaporation rates, and significant reductions in overall water availability. This shift is expected to intensify water scarcity during dry seasons, reducing the reliability of hydropower generation and increasing the frequency of low-flow conditions, with more significant hydrological variability and both higher peak flows and lower base flows over time [5].

Historical data indicates that the warming rate in the LMRB is higher than the global average, with more pronounced warming in the LRB than in the MRB. Indeed, the upper LRB historical data indicates an increase of 0.6°C per decade. Precipitation patterns have also shifted, with increased precipitation in the wet season across the basin and contrasting changes during the dry season: wetter conditions in the LRB and drier conditions in the MRB. These changes have led to increased streamflow in the LRB while slightly decreasing in the MRB, with future projections suggesting a slight increase in streamflow across the LMRB (see Figure 3) [1]. The lower MRB is expected to experience more significant precipitation variability with wetter and drier dry seasons. This region has seen historical decreases in streamflow during the wet season but increases during the dry season due to dam operations. Increased flood risks are projected due to higher precipitation and runoff during the wet season, and sediment management will become a major concern. The use of advanced simulation models, such as the WaterGAP2 model forced by multiple Global Climate Model (GCM), shows that projected increases in runoff could lead to promising changes in hydropower potential but require careful management of water resources to optimize electricity generation [5].

High Mountain Asia (HMA), including parts of the Lancang River's headwaters, is experiencing rapid climate change at rates double the global average. This rapid warming significantly impacts hydropower systems due to increased glacial melt and changes in seasonal runoff patterns. Critical threats include glacial retreat and permafrost thaw, leading to slope instability, glacier detachments, rock-ice avalanches, landslides, floods, and debris flows, all of which threaten the structural integrity and safety of hydropower projects [6].

Lastly, the LMRB's hydrological response to climate factors shows that climate change and human activity have substantially altered streamflow, leading to more frequent extreme events and a longer dry season. The LRB's hydrological response is more sensitive to climate factors than the MRB, demonstrating the accelerating impacts of intensive human activities. Before 2010, climate change was the critical driver of streamflow changes,

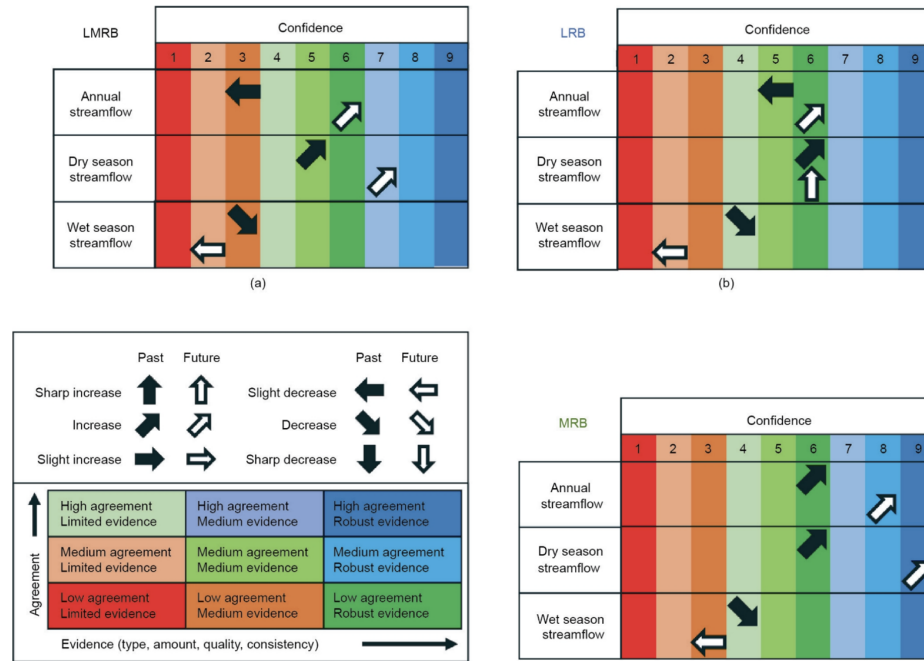


Figure 3: Projected changes in streamflow over (a) the LMRB, (b) the LRB, and (c) the MRB [1]

contributing 82.3% to variations from 1992 to 2009. However, after 2010, human activities became the dominant factor, contributing 61.9% from 2010 to 2014. Thus, while climate change continues to influence hydrology, the construction of dams and other human interventions significantly impact the region's water resources. Dam operations have also been shown to mitigate some of the variability in streamflow by regulating flows, increasing dry season flows, and decreasing wet season flows. However, this regulation also reduces the natural seasonality of river flows, impacting aquatic ecosystems [1].

### 2.1.2 Temperature Changes and Evaporation Rates

Rising temperatures are another critical factor impacting hydropower efficiency. The World Bank projects that average temperatures in Southeast Asia could increase by 2.5°C to 4.0°C by 2100 under a high-emission scenario [3]. Higher temperatures can increase reservoir evaporation rates, reducing the overall water volume available for energy production. It can be particularly problematic in tropical regions like Southeast Asia, where high temperatures are common year-round [2]. Increased evaporation not only diminishes water levels but also raises the temperature of the remaining water, affecting the cooling processes essential for turbine operation [1].

Studies indicate that evaporation losses in large reservoirs in the Mekong Basin could rise by up to 20% by 2050, significantly impacting hydropower production [1]. Effective strategies to mitigate evaporation losses include using floating solar panels, which can reduce evaporation by up to 70% while generating additional solar power, creating a synergistic effect that enhances overall energy output [7].

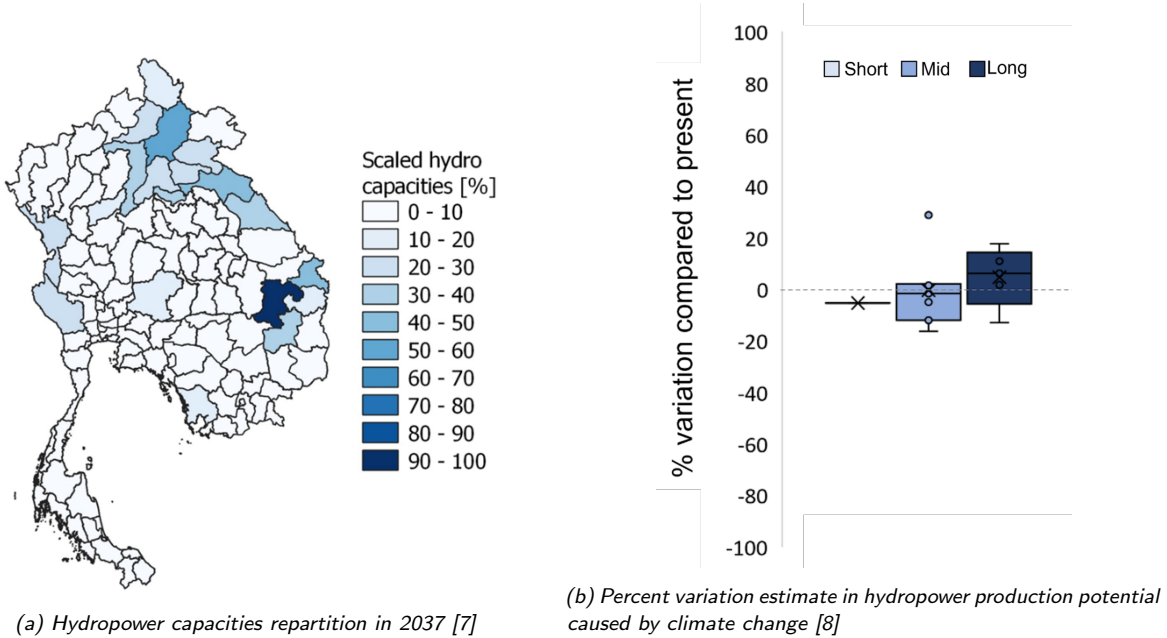


Figure 4: Projections for hydropower in Southeast Asia

### 2.1.3 Sedimentation and Reservoir Siltation

Enhanced erosion and sediment transport due to changing weather patterns and increased rainfall intensity lead to more significant sediment deposition in reservoirs. Sedimentation reduces dams' storage capacity and operational lifespan by clogging turbines and reducing the effective volume of reservoirs [9]. This process, known as reservoir siltation, can significantly diminish the efficiency and output of hydropower plants, necessitating frequent and costly dredging operations to maintain capacity.

In the Mekong River, sediment loads have increased by 30% over the past two decades due to deforestation and agricultural expansion, exacerbating the impacts of climate change [10]. Laos, which relies on hydropower for 90% of its electricity generation, has reported annual maintenance costs related to sedimentation exceeding \$10 million [1]. Effective sediment management strategies, including constructing sediment bypass systems and periodic dredging, are essential to mitigate these impacts and ensure the long-term viability of hydropower projects in the region [9].

### 2.1.4 Economic Impact

The economic implications of climate-induced variability in hydropower output are significant. Reduced hydropower output during droughts can increase reliance on fossil fuels, driving up operational costs and greenhouse gas emissions [11]. For example, during the 2016 drought, Vietnam had to increase coal imports by 30% to compensate for the reduced hydropower output, resulting in an estimated additional cost of \$500 million [2].

Additionally, the need for infrastructure repairs and upgrades due to damage from

extreme weather events further strains financial resources. The Asian Development Bank estimates that Southeast Asia will need to invest approximately \$3.1 billion annually in climate-resilient infrastructure, including hydropower, to cope with the impacts of climate change [12]. During periods of low water availability, countries like Laos and Cambodia may be forced to import electricity at higher costs, impacting national budgets and energy security [1].

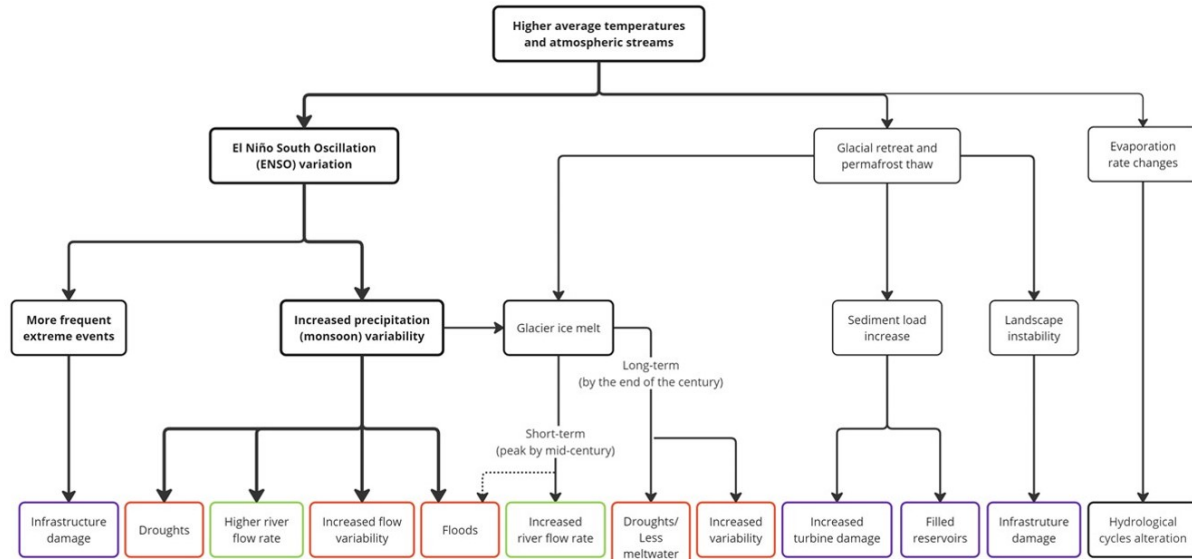


*Figure 5: Climate change impact on hydropower (the importance of a phenomenon is related to the width of its arrow and box)*

## 2.2 Solar Power

Solar power is emerging as a crucial component of Southeast Asia's energy landscape, especially in countries like Vietnam, Thailand, and Indonesia. The region's high solar irradiance and rapidly growing energy demands make it an ideal candidate for solar photovoltaic (PV) technology. With ambitious renewable energy targets, Southeast Asian nations are integrating solar power into their energy mix to enhance sustainability, energy security, and economic growth. Indeed, Vietnam aims to increase its solar capacity to 20 GW by 2030, making solar power a significant part of its energy portfolio [13]. Similarly, Thailand and Indonesia aim to generate 30% and 23% of their energy from renewables by 2036 and 2025, respectively, with solar power constituting a significant share of this transition [14]. Despite its potential, the viability and efficiency of solar power in Southeast Asia are influenced by various factors, including climatic conditions, technological advancements, and economic considerations. Understanding these factors' impact and importance is critical to developing and predicting solar power potential.

### 2.2.1 Temperature Variations

The operational efficiency of solar PV systems is highly sensitive to ambient temperature changes, which can affect output levels and the lifespan of solar equipment. A temperature

rise is typically associated with decreased PV efficiency, with potential reductions in panel efficiency by approximately 0.4% to 0.5% for every degree Celsius increase [11]. A detailed techno-economic assessment in Malaysia reveals that a temperature increase from 25°C to 35°C could reduce PV efficiency by up to 5% [15]. Higher temperatures also accelerate the degradation of PV materials, reducing their operational lifespans and increasing maintenance costs [11]. Climate change thus increases the need for innovative cooling technologies and heat-resistant materials to mitigate the adverse effects of elevated temperatures on solar panels [16].

## **2.2.2 Solar Irradiance and Weather Extremes**

Solar irradiance is a critical factor for solar energy production, but climate change can significantly alter irradiance patterns through changes in cloud cover, atmospheric composition, and extreme weather events. Projections indicate that cloud cover could increase by 10-20% in some Southeast Asian regions by 2050, potentially reducing the effectiveness of solar installations [7]. Additionally, extreme weather events such as typhoons and heavy storms pose substantial risks to solar infrastructure. For example, the Philippines, experiencing an average of 20 typhoons annually, faces significant damage to solar farms from these events [11]. The 2013 Typhoon Haiyan highlighted the vulnerability of solar installations to extreme weather, causing extensive damage to energy infrastructure [9]. Due to geographic and climatic diversity, the potential for solar power in Southeast Asia varies significantly across regions.

Vietnam's solar potential is unevenly distributed across its territory. The southern and central regions, particularly Ninh Thuan and Binh Thuan, exhibit the highest annual solar irradiance levels, exceeding 5 kWh/m<sup>2</sup>/day [13]. Southern Vietnam is expected to maintain high solar potential due to consistently high irradiance levels and relatively stable weather patterns conducive to large-scale solar farm installations. The Mekong Delta also offers significant potential due to its flat terrain and high solar irradiance, although concerns about land use and agricultural displacement need to be addressed [12]. Northern Vietnam, on the other hand, may experience more significant reductions in solar output due to increased cloud cover and frequent extreme weather events [11]. Climate models suggest that the region could see a substantial increase in cloudy days, potentially reducing solar irradiance by 10-15% by mid-century [7].

Thailand's solar energy potential is concentrated in the northeastern and central regions, where average solar radiation levels reach around 5.5 kWh/m<sup>2</sup>/day [14] with low cloud cover and stable climatic conditions. Projections indicate that the northeastern region may maintain stable solar irradiance levels, with minimal increases in cloud cover expected [17]. In contrast, the central and southern regions could experience more variability in solar irradiance due to seasonal monsoon patterns. During the monsoon season, cloud cover and rainfall can significantly reduce solar energy output. However, these effects are expected to be temporary and confined mainly to specific months of the year [7].

Indonesia's solar potential is geographically dispersed across its many islands, with regions such as Java, Bali, and Nusa Tenggara showing the highest potential, averaging 4.8 to 5.2 kWh/m<sup>2</sup>/day [14]. The archipelagic nature of Indonesia presents unique challenges and opportunities for decentralized solar energy systems. While Java presents significant opportunities for rooftop solar installations and small-scale solar farms, frequent volcanic activity and associated ash clouds can intermittently reduce solar irradiance [15]. Bali and Nusa Tenggara, with more stable weather patterns, are expected to experience less climatic disruption, making them more suitable for solar installations and microgrids [14].

The Philippines has substantial solar potential, especially in the central and northern regions, which receive high solar radiation levels. However, the country's vulnerability to typhoons poses a significant risk to solar infrastructure, including prolonged downtime and high repair costs [11]. Projections suggest that climate change could increase the frequency and intensity of typhoons, further exacerbating these risks. Developing typhoon-resistant solar panel designs and robust mounting systems is crucial to mitigate these risks [9].

Malaysia's solar potential is predominantly found in the peninsular region, where solar radiation levels are consistently high throughout the year. However, rising temperatures and increased rainfall could compromise solar potential, affecting panel efficiency and maintenance needs [18]. Increased rainfall can lead to higher humidity levels, affecting the performance and longevity of solar panels. Innovative approaches, such as using floating solar panels on water bodies, are being explored to maximize land use efficiency and minimize environmental impact [15].

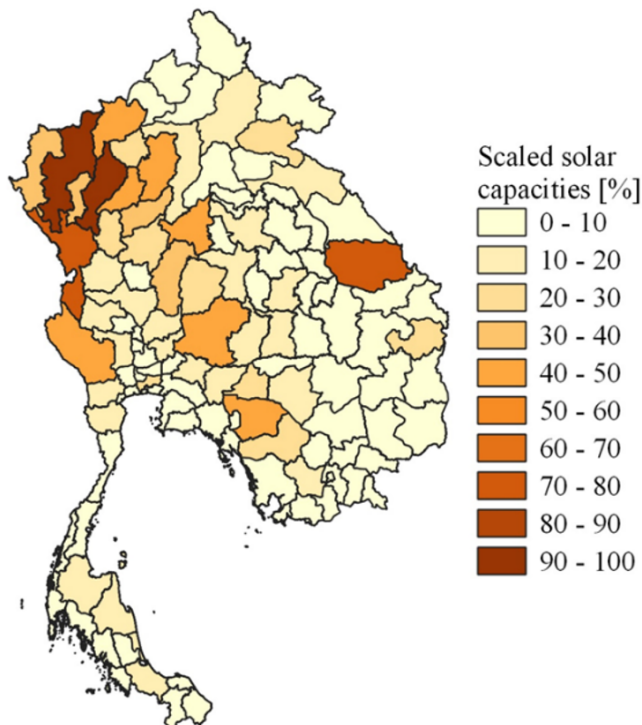


*Figure 6: Solar power capacities repartition in 2037 over continental Southeast Asia [7]*

### **2.2.3 Sea-Level Rise and Coastal Installations**

The threat of sea-level rise is particularly pertinent for coastal solar installations across Southeast Asia. Projections suggest a rise of up to one meter by 2100, which could inundate significant portions of coastal solar farms, potentially leading to substantial losses in energy production and increased costs for protective measures [12]. A one-meter rise in sea level could inundate up to 10% of Vietnam's solar farm area, leading to significant losses in energy production and increased costs for protective measures [19]. It underscores the necessity for strategic planning in site selection, resilient infrastructure design, and adaptive measures to protect solar investments from the impacts of rising sea levels.

### **2.2.4 Economic Viability**

The economic viability of solar projects in Southeast Asia hinges on the declining costs of solar PV technology and the management of climate-related risks, making it increasingly competitive with traditional energy sources [11]. While initial capital expenditure for solar installations remains high, operational and maintenance costs are low due to minimal maintenance needs and zero fuel costs. However, regions with high temperatures and humidity, such as Malaysia, face additional maintenance costs due to panel degradation and efficiency losses [19].

Climatic variability poses significant economic challenges to solar projects. Increased cloud cover or particulate matter can reduce solar irradiance, lowering energy output and financial returns. For instance, a 10% reduction in solar irradiance due to increased cloudiness can reduce annual energy output by approximately 10%, significantly impacting the profitability of solar energy systems [7]. To mitigate these risks, robust economic models that account for production variability and incorporate risk management strategies and energy storage systems are essential [14].

### **2.2.5 Technological Advancements and Infrastructure Development**

Technological advancements in solar PV systems, including improvements in panel efficiency and the development of bifacial and perovskite solar cells, are enhancing the viability of solar power in Southeast Asia. Current commercially available PV panels have efficiencies ranging from 15% to 22%. Emerging technologies like perovskite solar cells are expected to push efficiencies beyond 25%, significantly increasing the energy yield per unit area [14].

Infrastructure development, particularly grid modernization and the integration of energy storage systems, is crucial for supporting the expansion of solar power. Countries like Vietnam and Thailand are investing heavily in grid infrastructure to accommodate the intermittent nature of solar energy and ensure reliable electricity supply [13]. Additionally, floating solar PV installations on reservoirs and water bodies are gaining traction as a solution to land constraints and high evaporation rates, creating a synergistic effect by generating solar power while reducing water loss [7].

## **2.3 Wind Power**

Wind power is becoming integral to Southeast Asia's renewable energy strategy, driven by the region's growing energy demands and the need for sustainable energy solutions. Vietnam, Thailand, and Indonesia have set ambitious targets for wind energy to reduce their reliance on fossil fuels and enhance energy security. Vietnam plans to increase its wind power capacity to 6 GW by 2030 [14], and Thailand and Indonesia are making significant investments in wind energy to diversify their energy portfolios and meet their renewable energy targets [16]. However, climate change poses substantial threats to the sustainability and efficiency of wind power, which is highly dependent on climatic conditions, including wind speed, direction, and seasonal variability.

### **2.3.1 Wind Patterns and Speed Changes**

Wind power generation is intricately tied to climatic conditions such as wind speed, direction, and seasonal variations. Climate change presents both opportunities and challenges for wind energy in Southeast Asia. Higher wind speeds generally result in greater energy output from wind turbines. However, changes in atmospheric circulation due to global warming could lead to notable shifts in wind patterns across Southeast Asia. According to the IPCC, annual mean wind speeds could decrease by up to 10% in some areas while increasing by a similar margin in others by 2050 [3]. Global climate phenomena like the El Niño-Southern Oscillation (ENSO) could modify wind speeds [16]. Indeed, during El Niño events, some Southeast Asian areas may see increased wind speeds, enhancing wind power potential, while La Niña events might reduce wind speeds, diminishing energy output.

Seasonal and diurnal variations significantly influence wind power generation. Monsoon seasons in Southeast Asia bring strong winds that can enhance wind energy production. The Southwest Monsoon, occurring from May to September, increases wind speeds to an average of 6.5 to 7.5 m/s in Vietnam's coastal regions, boosting energy output during these months [13]. However, these seasonal variations can also cause increased wear on wind turbines due to high wind speeds and storm events [11]. Diurnal variations, with wind speeds fluctuating daily and night, necessitate integrating energy storage systems to ensure a stable power supply.

### **2.3.2 Extreme Weather Events**

Increased storm frequency and intensity pose significant risks to wind power infrastructure. Typhoons and heavy storms can cause severe damage to wind turbines, leading to high repair costs and prolonged downtimes. The Philippines, experiencing an average of 20 typhoons annually, faces significant risks to its wind infrastructure, with potential damages costing up to \$1 billion annually [11]. Robust engineering designs and improved forecasting methods are essential to mitigate these risks and enhance the resilience of wind energy systems.

### **2.3.3 Sea-Level Rise and Coastal Erosion**

The threat of sea-level rise is particularly pertinent for offshore wind installations. Projections suggest a rise of up to one meter by 2100, which could inundate significant portions of coastal infrastructure. Offshore wind projects, particularly in regions like the South China Sea, must account for these changes by designing resilient infrastructure [17]. In the case of Vietnam, a one-meter rise in sea level could impact up to 10% of the country's wind farm areas, necessitating adaptive measures to safeguard these investments [19].

### **2.3.4 Wind Power Potential Projections**

A study using the CORDEX-SEA regional climate model projects that the impact of climate change will differ geographically. Certain areas, such as the South China Sea, may experience a reduction in wind speed by 5-8% by mid-century, under high-emission scenarios, decreasing energy output from wind turbines. Conversely, northern regions of the Philippines might see an increase in wind speeds, potentially enhancing wind power potential but also posing challenges related to turbine design and durability [11].

Due to climate change, Vietnam's wind power potential is expected to evolve significantly. Coastal regions like Ninh Thuan and Binh Thuan have average wind speeds exceeding 6.5 m/s at 100 meters height and an estimated technical potential of 24 GW [13]. However, climate projections indicate that wind speeds in these areas could increase slightly during the monsoon season, further enhancing their potential [12]. Conversely, inland areas may experience more variability, potentially impacting the reliability of wind power generation.

Thailand's wind energy potential is concentrated in the central and northeastern regions, with average wind speeds around 5.5 to 6.0 m/s at 100 meters height and a technical potential of approximately 13 GW [14]. Future climate models suggest that these regions may maintain stable wind speeds, but increased variability during certain seasons could challenge consistent energy output [7]. Implementing advanced forecasting and energy storage systems will be crucial to mitigate these effects.

Indonesia's wind potential is geographically diverse, with regions like South Sulawesi and West Nusa Tenggara showing the highest potential, averaging 5.0 to 6.0 m/s at 100 meters height and a technical potential of 9 GW [14]. Climate projections indicate that these areas may experience increased wind speeds during El Niño events and more significant variability during La Niña events [16]. Developing resilient wind turbine designs and adaptive management strategies will be essential to harness this potential.

The Philippines has significant wind power potential, especially in the northern and central regions, where wind speeds average 6.0 to 7.0 m/s at 100 meters height, contributing to a technical potential of 76 GW [16]. Climate projections suggest that these regions may increase wind speeds due to shifting monsoon patterns, potentially enhancing wind power

potential [11]. However, the increased frequency and intensity of typhoons pose substantial risks to wind infrastructure, necessitating robust design and construction standards to withstand extreme weather events.

Malaysia's wind potential is relatively low compared to its solar potential, with average wind speeds of 3.0 to 4.0 m/s at 100 meters height in most regions. However, offshore wind projects, particularly in the South China Sea, show promise due to higher wind speeds and consistent wind patterns, offering a potential capacity of 20 GW [17]. Climate models indicate that offshore wind speeds may remain stable or slightly increase, making these areas viable for future wind power development.

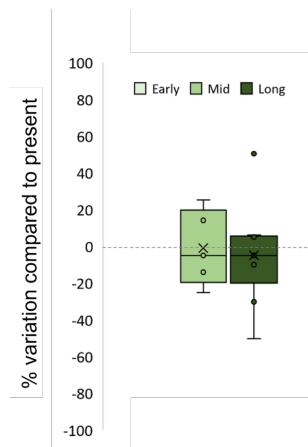


*Figure 7: Percent variation estimate in hydropower production potential caused by climate change [8]*

### 2.3.5 Economic Viability

The economic viability of wind power in Southeast Asia depends on various factors, including installation costs, maintenance expenses, and the ability to manage climate-related risks. The cost of wind technology has decreased significantly over the past decade, making wind power more competitive. The average cost of wind turbines has fallen from \$1,600 per kW in 2010 to \$1,200 per kW in 2020, driven by technological advances and economies of scale [14]. However, installation costs can be high, particularly for offshore wind projects, requiring substantial infrastructure and grid connection investments. For example, offshore wind projects in the South China Sea have installation costs ranging from \$3,000 to \$5,000 per kW, reflecting the higher complexity and logistical challenges of these installations [17].

While wind turbines have relatively low operational costs, maintenance expenses can be significant, especially in regions prone to extreme weather conditions. Regular maintenance is crucial to ensure the longevity and efficiency of wind turbines, with costs averaging \$50,000 per year for onshore turbines and \$100,000 per year for offshore turbines [16]. Climatic variability poses challenges to the economic viability of wind projects. Changes in wind patterns and increased storm activity can lead to inconsistent energy output and higher maintenance costs. Developing robust economic models and risk management

strategies is essential to mitigate these impacts and ensure the financial sustainability of wind energy projects [11].

## **2.4 Knowledge Gaps and Research Needs**

Despite advancements in understanding climate change's impacts on renewable energy, notable knowledge gaps persist. Many studies lack the granularity needed for accurate regional projections, which is essential for effective planning and adaptation. More precise climate models are necessary to predict regional climate changes and their specific effects on renewable energy resources, as current models often lack sufficient resolution. The role of the ENSO phenomenon in affecting renewable energy production requires a more detailed study. ENSO significantly influences weather patterns in Southeast Asia, with El Niño and La Niña events causing severe droughts and floods, respectively. Understanding how these events interact with long-term climate trends is crucial for developing robust adaptation strategies.

Long-term performance data for renewable energy systems under varying climate conditions are also insufficient. Comprehensive longitudinal studies monitoring solar, wind, and hydropower installations under different climate scenarios are essential for developing robust adaptation strategies. Additionally, interdisciplinary research combining climate science, engineering, and social sciences is needed to address the multifaceted challenges of climate change, including understanding the socio-economic impacts of climate-induced variability in renewable energy production and developing integrated solutions.

Existing literature often focuses on broad regional trends without addressing local variations in climate impacts and hydrological responses (see Figure 8). For instance, the heterogeneity within the Mekong River Basin regarding precipitation and runoff patterns is often oversimplified, leading to generalized conclusions that may not apply uniformly across the basin. The interaction between climate change and human activities, such as dam construction and deforestation, is frequently underexplored, yet crucial as human interventions can exacerbate or mitigate climate variability impacts. While trends in renewable energy production under climate change have been quantitatively investigated, their variability remains underexplored. Quantifying this variability is critical for designing resilient renewable energy systems capable of withstanding unpredictable climate impacts. Projections using RCP provide valuable insights but often lack localization. Climate models that consider specific regions' unique geographical and climatic conditions are needed.

Finally, the literature underrepresents the potential for adaptive strategies, such as integrating floating solar panels to reduce evaporation losses. Future research should address these gaps to provide a nuanced understanding of hydropower sustainability under changing climatic conditions.

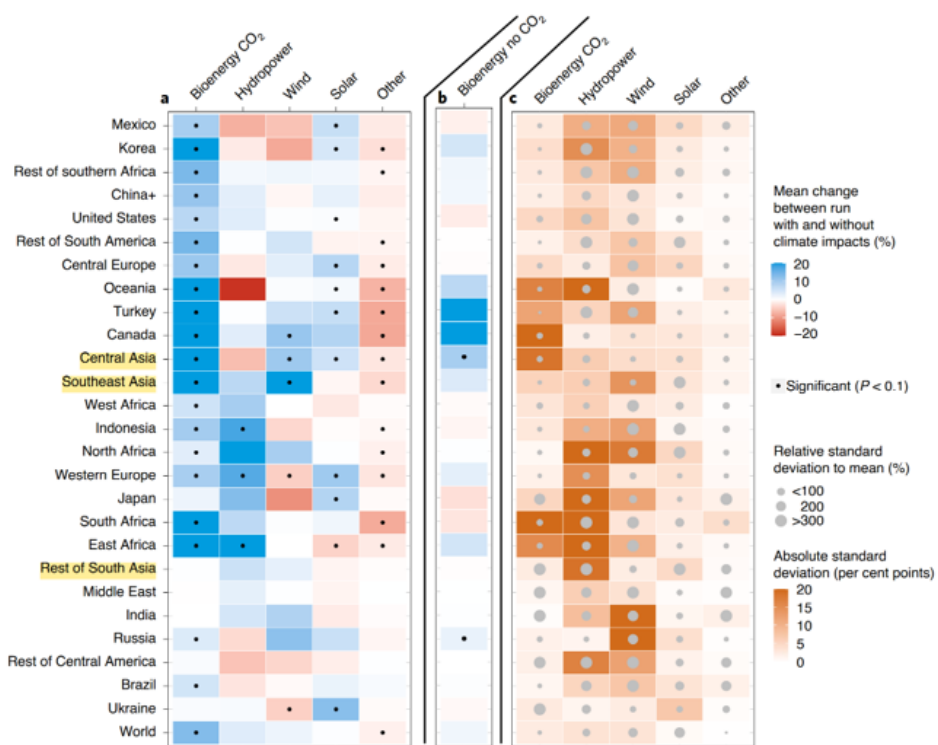


Figure 8: Combined relative effect of climate impacts on cumulative primary energy supply for each iMaGE model region. China+ includes Taiwan. [20]

### 3 General Approach and Methodology

#### 3.1 Research Project Orientation

This project aims to quantify the potential of renewables over a 40-year horizon. The primary variable under study is the minimum power generation at all times, as it defines the risk of power outages and disruptions. It requires an in-depth analysis of climate indices and power generation variability. While the literature review thoroughly panoramas the factors at stake for hydropower, solar power, and wind power generation in the context of climate change, it also highlights the lack of quantitative studies about power generation variability with high geographic granularity rather than general trends at a regional scale.

Thus, the main challenge the general project will tackle is evaluating renewable power potential variability at a high resolution in Southeast Asia to assess the risks of implementing generation installations at various regional locations and ensure maximum power production stability. In particular, it will involve quantifying the minimum power generation that can be expected with a high geographical granularity. This research project addresses the first step of this highly complex problem: identifying the necessary features to forecast the minimum power generation at specific locations for hydropower and design simple forecasting models.

#### 3.2 Methods and Materials

The initial phase of this project involved a detailed critical review of the existing literature on future renewable power generation in Southeast Asia. This review helped identify the primary factors influencing future renewable power production in the context of global warming. Understanding these factors is essential for feature selection, a critical step in preparing the training data for machine learning models designed to forecast future power generation. This research project specifically focuses on future hydropower generation as the initial phase of a broader initiative. Literature review indicates that the primary factors affecting hydropower generation include rainfall, temperature, and other climatic variables. Consequently, this study aims to determine how to effectively integrate these factors into forecasting models. As a river's flowrate and the potential hydropower generation of a hydropower plant on this river are linearly related (see Equations 1 and 2), this study focuses on forecasting flowrates rather than power generation. [14]

$$P = \eta \rho g H Q \quad (1)$$

$$H = \tan \alpha \times L \quad (2)$$

Where  $P$  is the power produced (W),  $\eta$  the "turbine + generator" efficiency,  $\rho$  the water density (kg/L),  $g$  the gravitational constant,  $H$  the hydropower plan head (m),  $Q$  the river discharge ( $m^3/s$ ),  $\alpha = \text{slope } (\circ)$ , and  $L = \text{average length of the diverted path (m)}$ .

The second stage of the project involves acquiring hydrological and climatic data from reliable sources to build a dataset. The data used in this project is from the Mekong River Commission (MRC) time series database. Daily data over the 2007-2024 period for rainfall (in millimeters) and flow rate (in cubic meters per second) at the Stung Treng measurement station are the base elements of the project dataset. These locations have been chosen for two primary reasons:

- a) daily data are available at this measurement station over more than 10 years.
- b) Stung Treng is located in the medium to lower part of the MRB, a region where Singapore is most likely to focus its renewable energy production efforts. Initiating the study at this strategic location provides a logical starting point before extending the forecasting models to the broader region. The underlying hypothesis is that the optimal feature selection and dataset preparation developed here can be generalized across the entire area.

The dataset also includes Cambodia's annual mean temperature and monthly average temperature data for each decade, sourced from the "Climate Change Knowledge Portal for Development Practitioners and Policy Makers." Thailand's annual Gross Domestic Product (GDP) between 2007 and 2023 from the International Monetary Fund (IMF) is added to the dataset to account for water pumpage in the Mekong, as the discharge is also impacted by agriculture and industry water extraction. Thailand is used because of the relative stability of its economy compared to other countries in the region. Vietnam's GDP has also been tested as a feature, but it showed no significant difference in forecast accuracy. Data was extracted and formatted into a usable structure using Pandas and Numpy libraries.

After constructing the dataset, the project is structured around two key studies: a statistical analysis of weekly and monthly data to explore correlations, trends, and variabilities among features and the selection and training of a machine learning model. The statistical analysis aims to identify reliable patterns and trends that can be used to extrapolate forecasts, potentially reducing the need for more complex machine learning models. Both components of the project are conducted using the Python programming language.

The statistical analysis involves extracting monthly and weekly minimum, average, and maximum discharge levels. Correlation matrices are visualized using Seaborn's `sns.heatmap` function to understand the relationships between features. The datasets constructed for this analysis include features such as "year", "week of year", "minimum flowrate", "maximum flowrate", "total rainfall over the week", "average rainfall over the week", and "average flowrate over the week", alongside "Thailand GDP". Missing data are addressed using second-order polynomial interpolation via `pd.interpolate()` from the Pandas library.

To further explore flowrate variations, TSD, autocorrelation, and partial autocor-

relation functions are applied to the minimum, maximum, and average flowrate features, as well as to the weekly average rainfall. The correlation functions are available in the `statsmodels.graphics.tsaplots` package. TSD analysis, performed using the `statsmodels.tsa.seasonal` library, helps discern seasonal patterns and trends within the data. Trends are extracted and loaded into a dataset to enable the same statistical and correlation analysis as with the raw data. Correlation coefficients with lagged features are also analyzed on both raw and decomposed data using `scipy.signal.correlate`. The objective is to identify significant patterns or correlations with rainfall data.

The second part of the project focuses on designing regression models to forecast future minimum discharge levels in Stung Treng. This involves comparing machine learning models, incorporating different features, to identify the most effective candidates. Simple models such as linear regressors and decision trees are employed to ensure the interpretability of the forecasting results. Random Forest and XGBoost regressors have also been implemented to compare accuracies. These modules are available in the Scikit-learn library.

Regarding data preparation, the models are trained on both raw data and data treated through TSD. In the first case, models are trained on raw data that has been scaled using `sklearn.preprocessing.StandardScaler`. The second approach involves extracting the trend, seasonal, and residual components of the scaled data using the `statsmodels.tsa.seasonal` library, and training regressors to predict future flowrate trends based on the rainfall trend data. The forecasted flowrate trend is then combined with the previously extracted flowrate seasonal pattern, thus recomposing a complete future discharge dataset (see Figure 9).

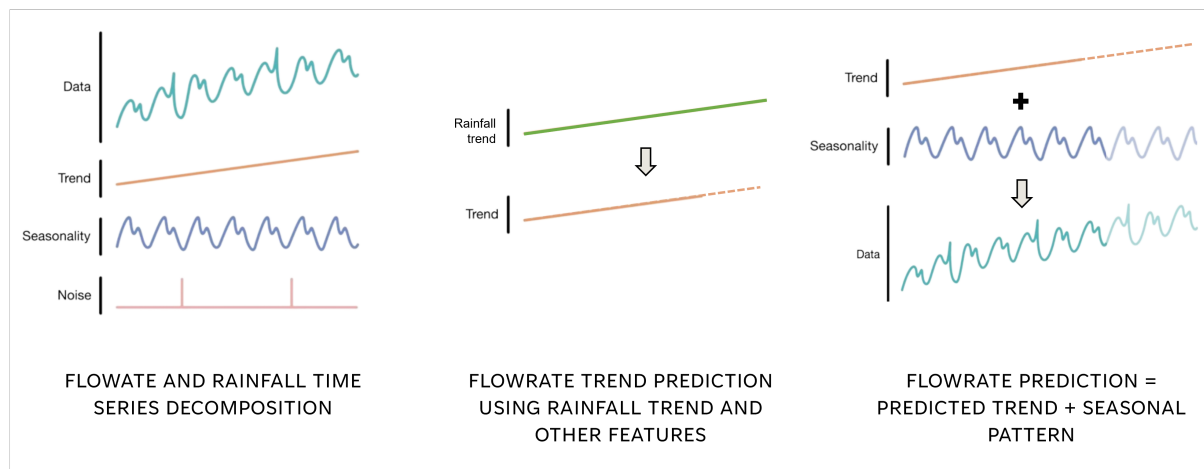


*Figure 9: Prediction methodology using TSD*

In both cases, polynomial features are introduced using the `PolynomialFeatures` function from the `sklearn.preprocessing` module. This technique enhances the model's capability to capture nonlinear relationships in the data, thereby facilitating more accurate predictions of future discharge levels based on the identified seasonal patterns and trends.

## 4 Results and Discussion

### 4.1 General statistics and analysis of monthly and weekly data

This first study serves as a preparatory stage for the predictive modeling that will be discussed in Section 4.2. In this section, we undertake a comprehensive statistical analysis of the monthly and weekly hydrological data, focusing on identifying key variables and establishing correlations crucial for feature selection in our regression models. This analysis is critical for selecting the most influential predictors and understanding their dynamics in relation to flowrate variations, which are fundamental for developing robust forecasting models.

#### 4.1.1 Average monthly data analysis

Functions are defined to compute monthly statistics, including minimum, maximum, average, and standard deviation of flowrates and average rainfall, as well as the GDP of Thailand and Vietnam. These statistics are applied to data averaged monthly over the years.

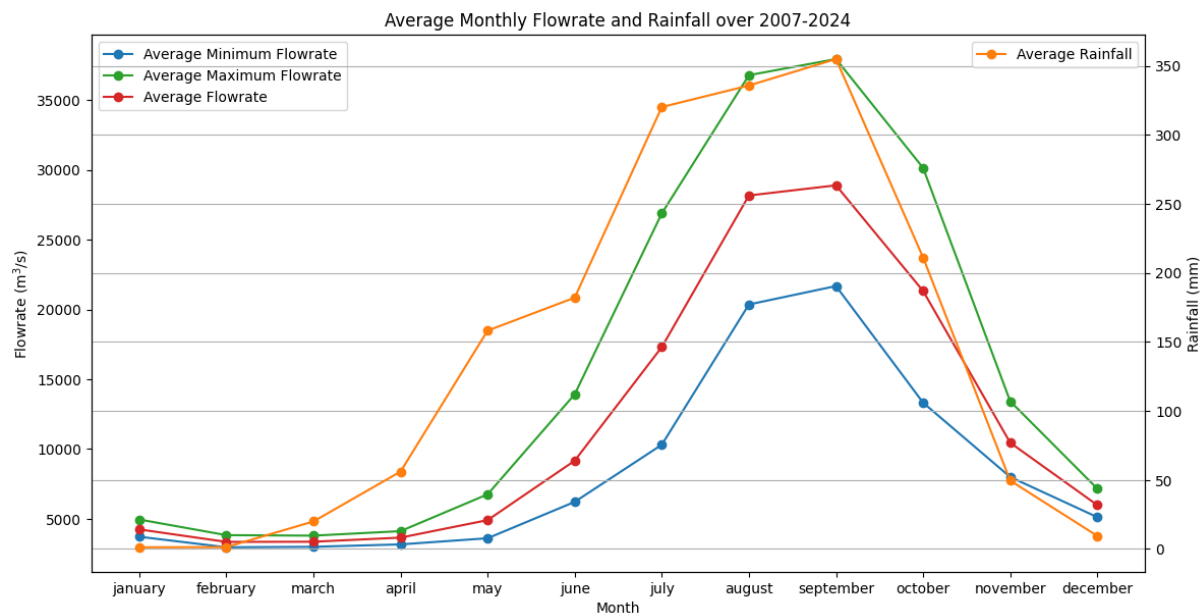


Figure 10: Average monthly flowrate and rainfall over 2007-2024 in Stung Treng

Figure 10 illustrates average monthly flow rates and rainfall in Stung Treng from 2007 to 2024, highlighting strong seasonal variations that are essential for hydrological modeling in Southeast Asia. The graph shows a pronounced correlation between rainfall and flow rates, with peaks during the monsoon months from May to October. This correlation suggests that rainfall significantly impacts river discharge levels, a key variable for predicting flow rates.

The consistent seasonal pattern observed in the data allows for the development of predictive models that use rainfall as a primary input to forecast future flow rates. By quantitatively modeling the relationship between rainfall and flow rates, we can predict seasonal variations in river discharge. This capability is crucial for the effective planning and management of hydropower resources, as it enables more accurate forecasting of water availability for energy production.

Additionally, the predictable nature of these seasonal trends supports applying statistical methods and machine learning algorithms to refine these predictive models. Accurately modeling this relationship is critical for optimizing hydropower operations and adapting to potential changes in rainfall patterns due to climate variability. This approach highlights the importance of integrating detailed climatic and hydrological data into energy management practices to ensure sustainable hydropower generation.

#### 4.1.2 Average weekly data analysis

The functions defined before are applied to weekly discharge data from 2007 to 2024 to create a new dataset. This new data is plotted to analyze yearly patterns and seasonality over the years (see Figure 11).

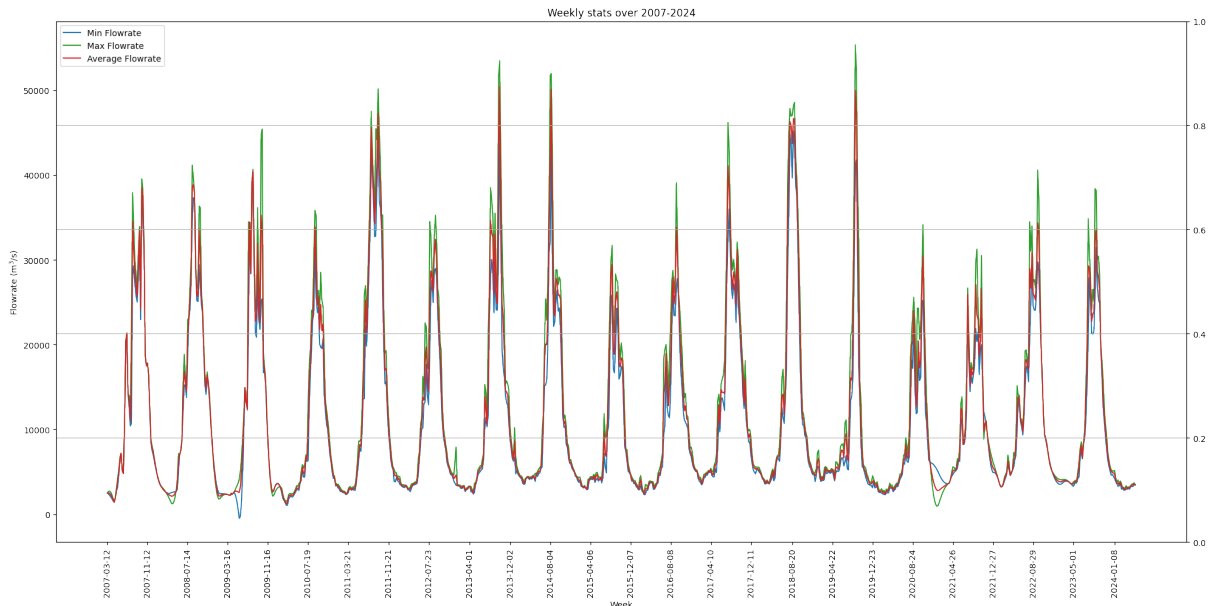


*Figure 11: Weekly discharge data over 2007-2024 in Stung Treng*

Figure 11 offers a detailed view of flow rate fluctuations weekly. This resolution captures the nuances of hydrological responses to weather events better than monthly data, highlighting trends and anomalies that are crucial for modeling hydrological dynamics while reducing the noise associated with daily data. The graph shows clear seasonal patterns with defined peaks during the monsoon periods and troughs in dry seasons, simplifying the modeling task since the data exhibit predictable cyclic behaviors. However, the presence of sharp spikes and rapid declines within these cycles suggests that extreme events and rapid changes are also captured, which could complicate modeling efforts.

These fluctuations require models that can either adapt to both gradual seasonal changes and abrupt hydrological responses to intense rainfall events.

To further understand rainfall and discharge data patterns and trends, TSD is applied to minimum, maximum, and average flowrates, as well as to the weekly rainfall average in Stung Treng to break them down into three components: trend, seasonal, and residual (Figure 12). The TSD of both rainfall and flowrate data distinctly exhibits the inherent seasonal patterns, substantiating the significant seasonal influence on hydrological behavior. All variables exhibit pronounced seasonal patterns indicative of specific periods characterized by consistently higher or lower values, aligning with expected seasonal climatic influences such as monsoons or snowmelt cycles. The trend components across these variables show moderate fluctuations without any distinct long-term upward or downward trends, suggesting a relative stability in the overarching patterns of rainfall and flowrates over the observed period. The residual plots, representing the unexplained variance after accounting for trend and seasonality, show minimal noise, indicating that the major fluctuations in the data can be attributed effectively to these components. This minimal residual variance underscores the adequacy of the seasonal and trend components in capturing the primary dynamics of the dataset.

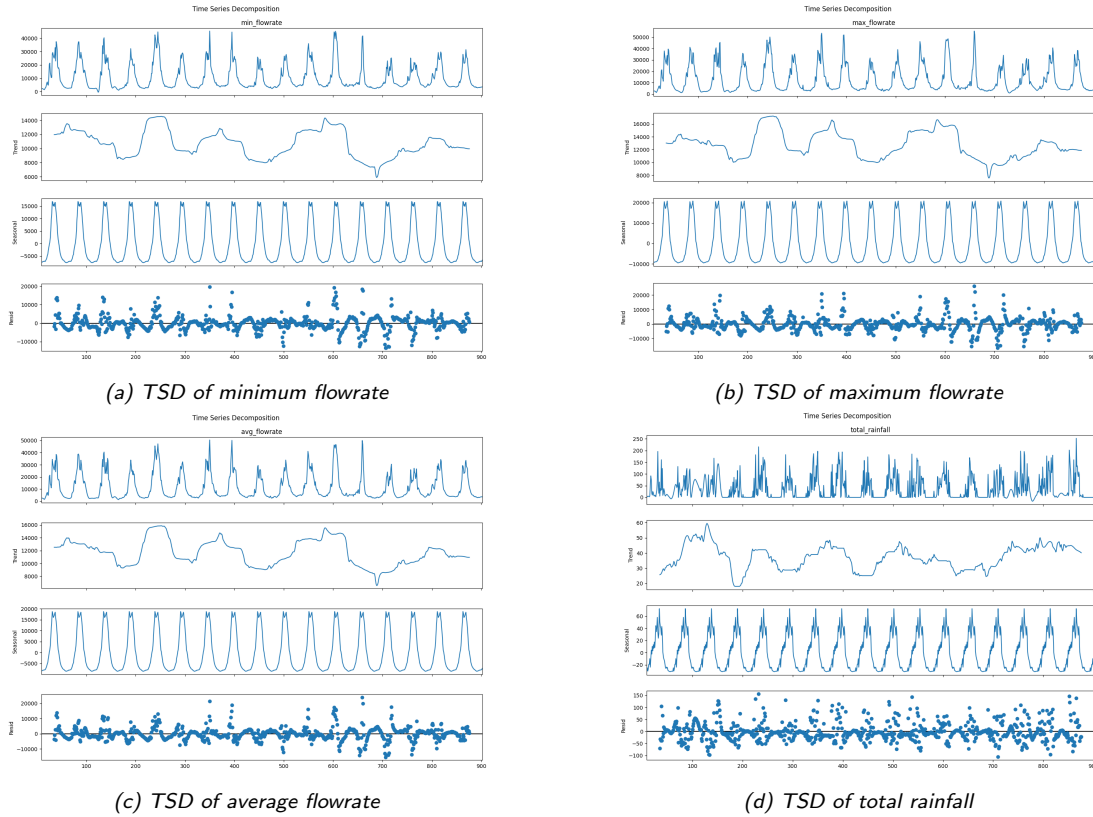


Figure 12: TSD of weekly minimum (a), maximum (b), average flowrates(c), and total rainfall (d) for Stung Treng data over 2007-2024

For predictive modeling, the strong seasonal correlation between rainfall and flowrates suggests that models should incorporate seasonal adjustments to enhance prediction accuracy. The similar timing and shape of the seasonal peaks across the variables suggest

potential direct relationships, possibly with lag effects where peak rainfall volumes may precede increased flowrates. Accurately modeling these relationships could involve using regression models with seasonal dummy variables to handle the explicit seasonal patterns observed or Seasonal Autoregressive Integrated Moving Average (SARIMA) models. Overall, the analysis indicates that with proper modeling of the observed seasonal patterns and potential lag effects, there is significant potential for accurately predicting minimum flowrate based on rainfall data.

Then, ACF and PACF plots in Figure 13 provide a deeper insight into the temporal dynamics of the data. Indeed, autocorrelation (also known as serial correlation) refers to the correlation of a signal with a delayed copy of itself as a function of delay. It is used to identify repeating patterns or periodic signals within datasets. Partial autocorrelation offers a refinement over autocorrelation by isolating the relationship between an observation at a particular time and its past observation at a lag, but only after removing the effects of their mutual correlations with other observations between them.

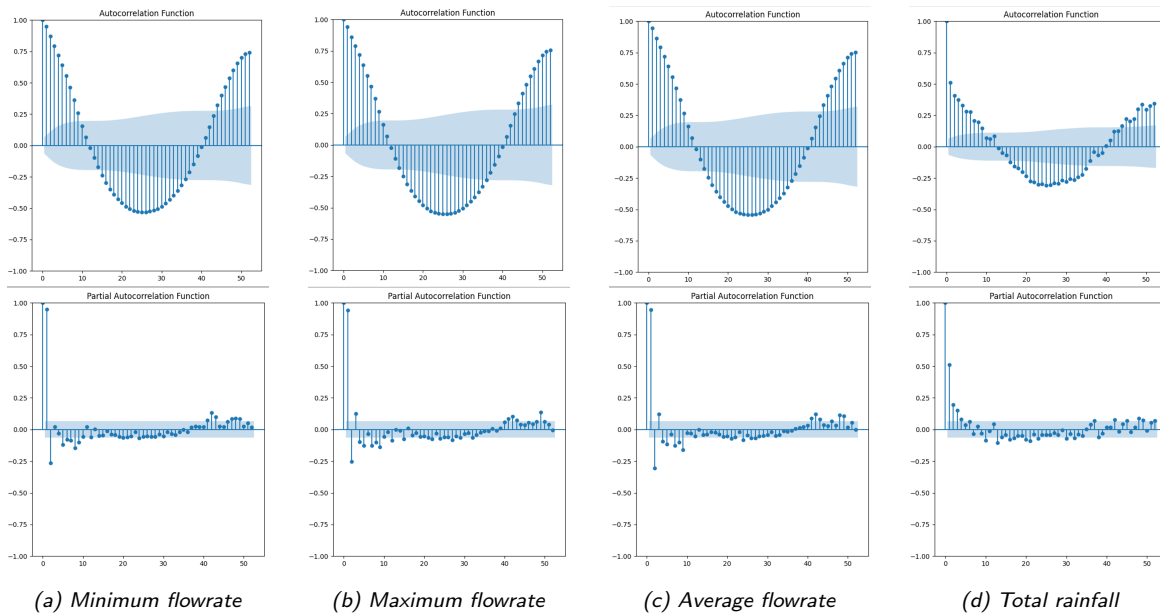


Figure 13: ACF and PACF of weekly minimum (a), maximum (b), average flowrates(c), and total rainfall (d) for Stung Treng data over 2007-2024

The ACFs demonstrate a robust cyclical pattern, suggesting a pronounced seasonality with potential predictability over short spans. This cyclic behavior implies that past data, particularly from the same season in previous years, may be critical for forecasting models. The flowrate PACFs decay in a sharp drop after 2 weeks, indicating that flowrate values are predominantly influenced by their immediate past values rather than long-term historical data. Rainfall PACF similarly shows strong initial correlations with a more gradual decline, suggesting a slightly prolonged influence on future values. The high initial spikes in PACFs suggest that regression models for predicting flowrates should prioritize short-term lag rainfall and flowrate features to capture the immediate hydrological response. Effective forecasting should focus on both the strong seasonality and the high predictiveness of recent past values, ensuring robust modeling of flowrates based on rainfall data.

After analyzing chronological patterns and data TSD, the next step is understanding correlations between hydrological and climatic features. In the pursuit of refining regression models for predicting flowrates based on rainfall data in the Stung Treng region, analyzing correlation matrices for both raw weekly data and their trends is imperative. The correlation heatmaps are plotted both for original data and trends in Figure 14. The correlation matrix for raw data demonstrates exceptionally high correlations among the different measures of flowrate: minimal, average, and maximal flowrates exhibit correlations exceeding 0.98. This indicates a potential redundancy in using all these variables simultaneously in predictive modeling, as they provide similar information.

Regarding the relationship between weekly rainfall and flowrates, the raw data matrix exhibits moderate correlations (0.49 with minimal flowrate and 0.52 with average flowrate). This moderate correlation suggests that while rainfall influences flowrate, it alone may not be a robust predictor for flowrate variations due to unaccounted external factors affecting flow dynamics, such as land use changes, water management practices, or seasonal variability in precipitation intensity and distribution.

Turning to the trends correlation matrix, similar patterns are observed, with strong correlations among the flowrate variables and moderate correlations between these flowrates and rainfall trends. The persistence of moderate correlations in the trends data indicates that the relationship between rainfall and flowrates, though significant, involves complex interactions likely influenced by delayed hydrological responses or accumulative effects not captured by simple linear models.

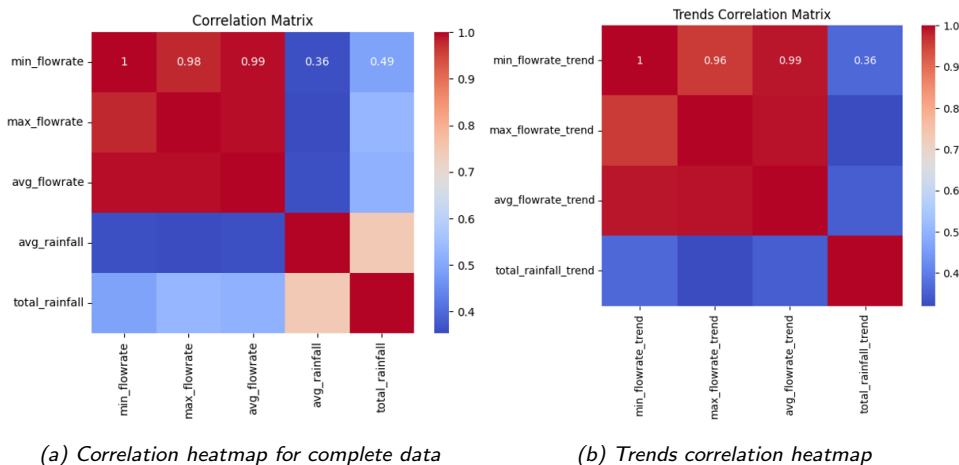
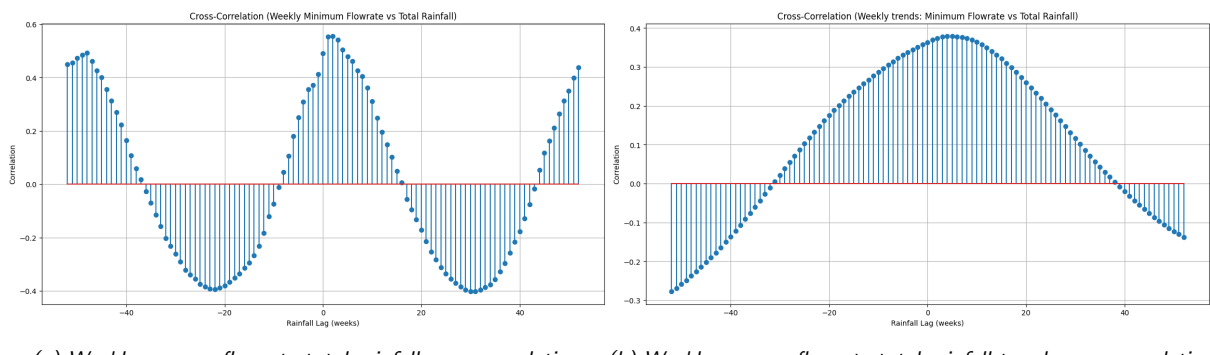


Figure 14: Correlation heatmaps for Stung Treng weekly data (avg = average, min = minimum, max = maximum)

For the next steps in regression modeling, these observations suggest focusing on integrating rainfall data with other potentially explanatory variables that could capture additional variability in flowrate responses. Exploring variables representing hydrological or climatic conditions, such as temperature, humidity, or evapotranspiration, could help capture the broader spectrum of environmental factors influencing flowrate dynamics. Additionally, considering hydrological lag effects by incorporating past rainfall data (e.g., rainfall totals over previous weeks or months) might improve model accuracy.

Therefore, to better understand the correlation between average flowrate and weekly total rainfall, including lag effects, cross-correlation analysis is done on raw data and trends in Figure 15. The reference used for this analysis is flowrate, and the lags are applied to rainfall data. Positive correlations around lag 0, with a peak correlation coefficient of approximately 0.6, imply that higher rainfall is directly associated with higher flow rates in the same period. The lag at -52 and +52 weeks further reinforces this annual periodicity, suggesting that the flowrate this year is influenced by the rainfall from the same time last year. The negative correlations around -26 and +26 weeks indicate that when there is high rainfall in one part of the year, there tends to be a lower flowrate approximately half a year later, highlighting the wet season/monsoon season cycle. The sustained high absolute value of correlation up to 10 weeks around lag 0 highlights the prolonged hydrological response to rainfall events. This suggests that after a rainfall event, the impact on flowrate persists for several weeks, indicating a lagged response in the hydrological system. This finding underscores the importance of incorporating lagged rainfall features up to this period to capture delayed flowrate responses, enhancing model accuracy in forecasting weekly flowrate changes. Moreover, trend cross-correlation analysis reveals a broader correlation peak around zero lag, stretching from -20 to +20 weeks, with a 0.36 peak correlation obtained around +5 weeks. Thus, adding more rainfall data lags to trend features can improve the models' performances significantly, especially around +5 weeks, even though the correlation is less important than for raw data. Therefore, trends can also be exploited as features in regression models, allowing a TSD approach for forecasting frameworks.



(a) Weekly average flowrate-total rainfall cross-correlation    (b) Weekly average flowrate-total rainfall trends cross-correlation

*Figure 15: Weekly average flowrate-total rainfall cross-correlation for Stung Treng data over 2007-2024*

In conclusion, the analysis of correlation heatmaps for both raw weekly data and trends revealed significant relationships that are essential for predictive modeling. We identified strong correlations between rainfall and both minimum and average flowrates, which are critical for forecasting river discharge. This detailed examination underscores the potential of rainfall as a prediction feature, indicating that it can be a robust independent variable in regression models to predict these specific flowrate metrics. The findings also highlight the importance of including lagged rainfall values in the model, as they exhibit high correlation coefficients for upcoming flowrate values. The immediate impact of rainfall on river discharge, reflected in short-term solid correlations, suggests that shorter lag periods might be crucial for accurate predictions. Finally, trends extracted from TSD can also

be exploited to predict flowrate as an alternative approach. These insights will guide the feature selection process in Section 4.2, focusing on developing robust regression models that use rainfall data to predict minimal and average flowrates effectively.

## 4.2 Discharge forecasting models

The objective is to select the best regressor and features to forecast future hydropower generation. The results of Section 4.1 allowed us to justify using rainfall data and lag data as features but also showed that the correlation with flowrate is not significant enough to ensure sufficient forecast accuracy. Thus, this section delves into implementing additional features and compares regressors' performance for various sets of features.

### 4.2.1 Models learning on original data

The first approach is to train regressors on the features selected among complete (i.e., non-decomposed) data. As maximum interpretability of the models is required, simple regressors like linear and decision tree regressors are preferred. In this subsection, the target used for every model is the weekly minimum flowrate.

#### Linear Regression models

First, linear regressors are assessed using the following features: rainfall with days and weeks lags (1-3 days & 1-10 weeks), mean rainfall over the past week, Thailand GDP, monthly and weekly minimum flowrate. Polynomial features are also added to the training set for some regressors via a second-order polynomial transformer. Four sets of features were tested, both with and without polynomial transformations, and are summarized in Table 1.

Feature	Set 1	Set 2	Set 3	Set 4
Rainfall	✓	✓	✓	✓
Week of the year	✓	✓	✓	✓
1-day rainfall lag	✓	✓		✓
2-day rainfall lag	✓	✓		✓
3-day rainfall lag	✓	✓		✓
5-week rainfall lag	✓	✓	✓	✓
Total weekly rainfall	✓	✓		✓
Min. flowrate of the week	✓		✓	
Min. flowrate of the month	✓		✓	
GDP				✓

*Table 1: Feature Sets for Linear Regression models*

The dataset is partitioned into training and testing sets using an 80-20 split. The training and testing sets are subsequently sorted by index to preserve any temporal

order inherent in the data. To rigorously evaluate the models' performance, 5-fold cross-validation is employed. It involves dividing the dataset into five equal subsets, training the models on four subsets, and validating them on the remaining subset. This process is repeated five times, allowing each subset to serve as the validation data once. The linear regression models are then trained on the whole training set and evaluated on the test set. The models' performances is assessed through Mean Squared Error (MSE) and  $R^2$  score, which provided measures of prediction error and the proportion of variance explained by the model, respectively. These evaluations ensured a comprehensive understanding of the model's predictive capabilities and generalizability.

The metrics for linear regressions are presented in Figure 2. At first view, it can be noted that the best-performing linear regression is the one based on Set 1, including all features. Polynomial transformation also increased the model's accuracy by  $3.10^{-3}$ . Additionally, the dataset uses only a 5-week rainfall lag as rainfall lag data performs almost as well as the one including all the available lag features. Thus, it allows us to consider using less complex rainfall projection models with only weekly resolution while conserving a comparable accuracy of river discharge projections. This result is coherent with the conclusions of the cross-correlation study led in Section 4.1. Also, it appears that adding a GDP feature does not significantly improve the regressor's accuracy. This may be due to a negligible human activity feature or a non-optimal index choice for water extraction. From now on, this feature will not be considered anymore to simplify the problem. A further study of future hydropower generation may want to investigate this aspect.

Linear Reg Model	MSE	$R^2$ score
Set 1 (Polynomial features)	0.045609	0.956969
Set 1	0.048403	0.954333
Set 3 (Polynomial features)	0.050693	0.952173
Set 3	0.055169	0.947950
Set 4 (Polynomial features)	0.419131	0.604560
Set 2 (Polynomial features)	0.430881	0.593474
Set 4	0.571429	0.460870
Set 2	0.578604	0.454101

*Table 2: Performance metrics of Linear Regression models*

Then, the best model is chosen to be studied on data sorted month by month to improve its performance. The selected model is thus Set 1. The chosen training dataset is trained both with and without polynomial transformation. The metrics of this training are shown in Table 3. Polynomial features are also tested but performed poorly compared to original features.

From these results, we can conclude that using monthly features significantly improved the regressions' performances for months from December to April but decreased the accuracy of the results for others like August, July, and October. It seems that the performances improved mainly for dry season months while deteriorating for monsoon

season months. It can also be noticed that using polynomial transformed features does not improve MSE, contrary to the previous results for whole-year training datasets.

Therefore, a more efficient approach could combine the two options: using the predictions from a regressor based on a complete training dataset and refining the flowrate projections of wet season months using monthly sorted datasets. This approach has not been studied yet in this project, but it could be an interesting extension to it.

However, the absence of a flowrate reference feature, as a minimum flowrate over the last week or month, causes the MSE to increase by a factor of 10 (as shown in Table 2). Thus, this regression model does not seem adequate for a projection model based on non-flowrate features. Such a model is needed in this project since including these flowrate features implies using the projections on rolling months, which is incompatible with long-term projections.

## Decision Tree regressors

After considering linear regressors, decision tree regressors were studied to compare their performances to the previously obtained ones, and their compatibility with models using only non-flowrate features was assessed. This regressor is chosen for its interpretability, which is a critical criterion in this project. Seven sets of features detailed in Table 4 are compared using decision trees.

Feature	Set 1	Set 2	Set 3	Set 4	Set 5	Set 6	Set 7
Rainfall	✓	✓	✓	✓	✓	✓	✓
Week of the year	✓	✓	✓	✓	✓	✓	✓
1-day rainfall lag	✓	✓	✓				
2-day rainfall lag	✓	✓	✓				
3-day rainfall lag	✓	✓	✓				
5-week rainfall lag	✓	✓	✓			✓	✓
Total weekly rainfall	✓	✓	✓	✓	✓	✓	✓
Min. flowrate of the week	✓	✓		✓		✓	
Min. flowrate of the month	✓		✓		✓		

Table 4: Feature Sets for Decision Tree models

Month	MSE	R <sup>2</sup> score
April	0.000415	0.94
March	0.000448	0.94
January	0.000451	0.93
February	0.000521	0.86
December	0.01141	0.94
November	0.05536	0.94
May	0.07433	0.77
June	0.03497	0.71
October	0.06617	0.89
August	0.10917	0.87
July	0.11575	0.85
September	0.15176	0.76

Table 3: Performance metrics of monthly Linear Regression models

The process is similar to the one detailed for linear regressors, but hyperparameter tuning is also conducted to optimize the Decision Tree regressors. A parameter grid is defined with ranges for `max_depth`, `min_samples_split`, `min_samples_leaf`, and `max_features`. Using GridSearchCV with 5-fold cross-validation, each combination of hyperparameters is evaluated based on the negative MSE. The best model is identified and trained on the training data, then used to predict the test set. The models' performances are evaluated using MSE and R<sup>2</sup> metrics. Table 5 presents the model comparison results.

<b>Model Description</b>	<b>MSE</b>	<b>R<sup>2</sup> score</b>
Set 6	0.046546	0.956085
Set 1	0.047975	0.954737
Set 2	0.056049	0.947119
Set 4	0.059667	0.943706
Set 3	0.115450	0.891076
Set 5	0.117438	0.889200
Set 7	0.238827	0.788825

*Table 5: Performance metrics of Decision Tree models*

The most accurate model is based on Set 6, followed by the Set 1 model using all available features. Therefore, including only the 5-week rainfall lag feature is more efficient than including all lag features, and a monthly baseline is not necessary when using a weekly baseline. These figures also show that non-flowrate features only do not allow us to achieve quality projection results with a MSE of 0.24.

Random Forest and XGBoost regressors are tested on the best feature sets to compare performances and test the accuracy expected with more complex models. Thus, the chosen datasets are Sets 1 and 6. The plot for the Random Forest model based on Set 1 is exhibited in Figure 16. The results in Table 6 demonstrate that implementing these regressors only improves accuracy by 10<sup>-2</sup> while making the models challenging to interpret. Therefore, the use of such regressors does not seem to be necessary for this project at this time.

<b>Model Description</b>	<b>MSE</b>	<b>R<sup>2</sup> score</b>
Random Forest (Set 1)	0.03734	0.964399
Random Forest (Set 6)	0.037921	0.964223
XGBoost (Set 6)	0.040909	0.961403
XGBoost (Set 1)	0.041252	0.961079

*Table 6: Performance metrics of Random Forest and XGBoost models trained on Sets 1 & 6*

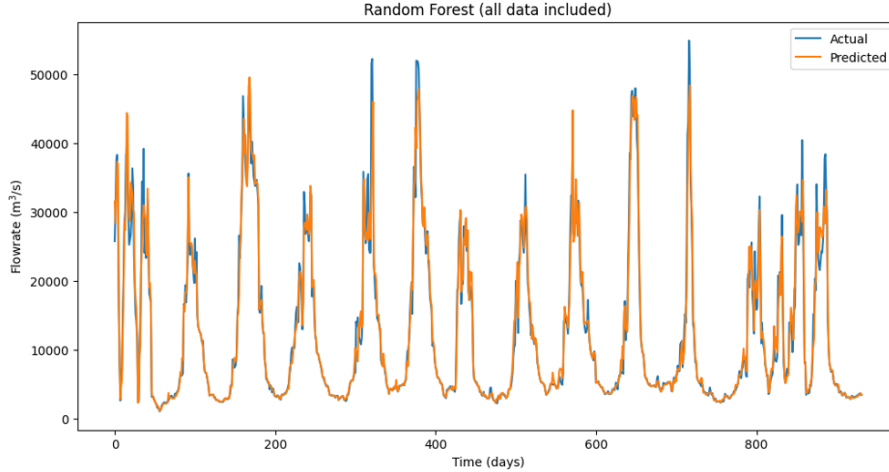


Figure 16: Random Forest model for Set 1

While the projections presented in the previous part seem relatively accurate, they still present a significant disadvantage in solving the problem at stake: the efficient ones use a "minimum flowrate of the week/month" feature, and the results show that removing the "past flowrate" feature greatly reduces the accuracy of the river discharge projections. Therefore, another approach is needed to overcome the need for a flowrate feature that is incompatible with this project's objective to make long-term flowrate projections.

#### 4.2.2 TSD Approach

The conclusions of Section 4.1 are promising regarding exploiting trends extracted from TSD for future flowrate projections. The approach adopted here is detailed in Methods and Materials (see Section ??). The first step is to extract the different components of rainfall and discharge data and log them to build a dataset. Classic TSD and Seasonal and Trend decomposition using Loess (locally weighted scatterplot smoothing) (STL) TSD (using `statsmodels.tsa.seasonal.seasonal_decompose` and `statsmodels.tsa.seasonal.STL`) are compared. Figure 17 shows the two decompositions obtained for flowrate. The seasonal component of STL decomposition is less regular as this decomposition seems to have more difficulty handling the discharge patterns after 2020. On the contrary, the classic TSD shows a regular pattern until 2022 for the seasonal component. So, initially, the classic decomposition seems more relevant as the basis for the projection models.

The goal is to make flowrate trend projections based mainly on rainfall trend features. Figure 18 presents the superposition of rainfall and flowrate trends for both decomposition methods.

The rainfall and discharge trends follow the same patterns for both decompositions but display relative amplitude variations. Correlation heatmaps are computed to quantify the correlation between these trends and justify the adopted approach. The correlation heatmaps for the features of both classic and STL TSD final datasets are displayed in

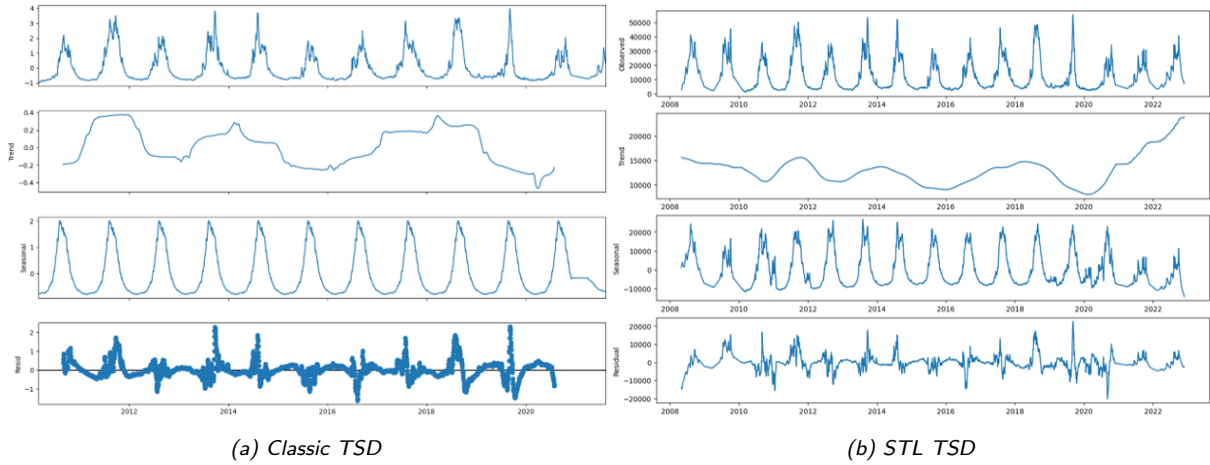


*Figure 17: Decomposition of Stung Treng flowrate data over 2007-2024*

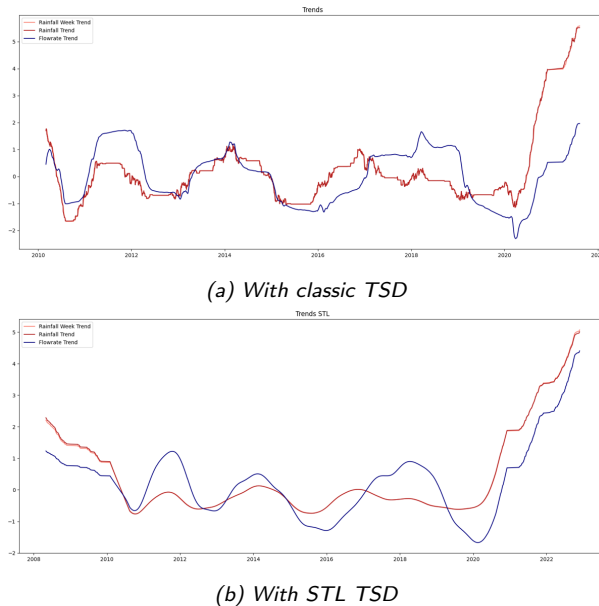
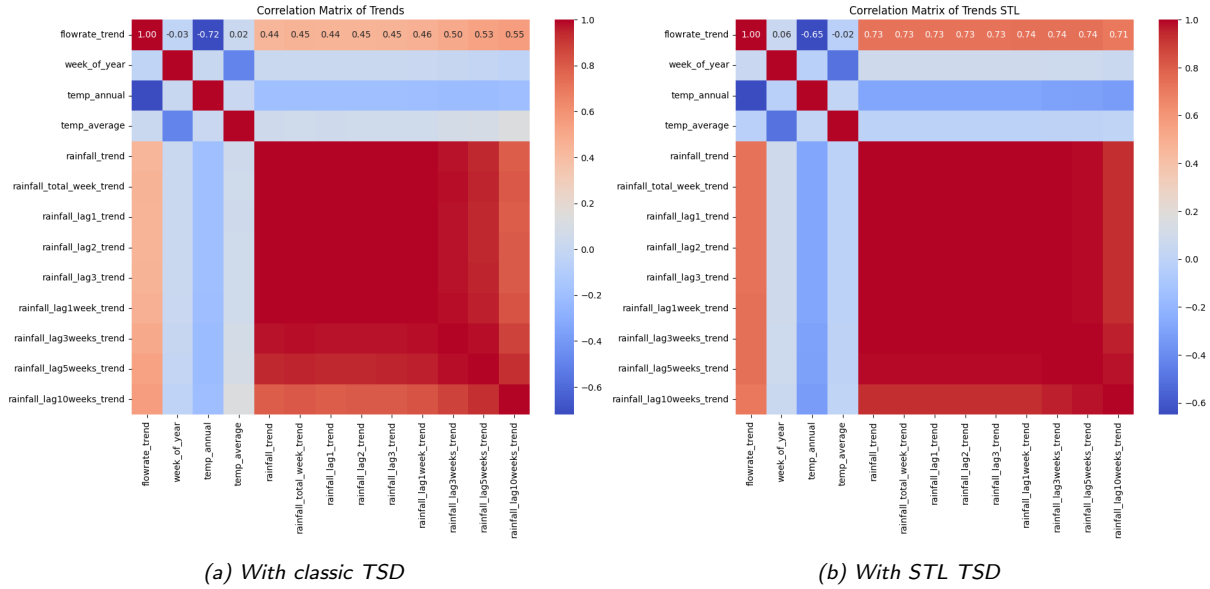


Figure 18: Trends for rainfall, flowrate, and weekly rainfall data in Stung Treng data over 2007-2024

Figure 19. In general, correlations between flowrate trend data and rainfall trends or other features are stronger or STL decomposition. The only exception is the monthly average temperature (`temp_average`). For classic TSD, the correlations are around 0.5, while they are around 0.73 for STL TSD. Thus, the approach seems more justified for the STL decomposition. It should also be noted that this result implies that all rainfall lag trends have comparable importance in the models and should be considered for the regressions. Still, this conclusion has to be put in perspective with the previous observations about the precision of STL TSD compared to classic TSD. STL decomposition is expected to produce a greater error due to the original decomposition process. In contrast, the classic decomposition is expected to induce a more significant error during the linear regression. Therefore, the rest of the study is led on both decompositions to compare their final performances regarding complete future flowrate projections.



*Figure 19: Trend features correlation heatmap*

In this study, four models are compared based on the above considerations, each of them trained on a dataset including the following features: 'rainfall trend', 'week of the year', 'mean annual temperature', 'monthly mean temperature', 'total weekly rainfall trend', '1-day rainfall lag trend', '2-day rainfall lag trend', '3-day rainfall lag trend', '1-week rainfall lag trend', '2-week rainfall lag trend', '3-week rainfall lag trend', '4-week rainfall lag trend', '5-week rainfall lag trend', '10-week rainfall lag trend', 'Thailand's GDP', 'Vietnam's GDP'. The target is the weekly minimum flowrate. The models are the following:

- Model 1: Linear regression on the dataset built with classic TSD
  - Model 2: Linear regression on the dataset built with classic TSD, with second-order polynomial feature transformation
  - Model 3: Linear regression on the dataset built with STL TSD
  - Model 4: Linear regression on the dataset built with STL TSD, with second-order polynomial feature transformation.

Model	MSE	R <sup>2</sup> score
Model 3	0.000 418	0.99
Model 4	0.050 184	0.95
Model 1	0.096 904	0.91
Model 2	0.248 772	0.75

*Table 7: Performance metrics of Trends Linear Regressions*

The performance metrics of these models are presented in Table 7, while the plotted curves can be found in Figure 20. The third model is by far the best-performing one, followed by the other model based on STL data decomposition as expected after the correlation analysis. Contrary to the results of the first approach, implementing polynomial transformation has not improved model accuracy.

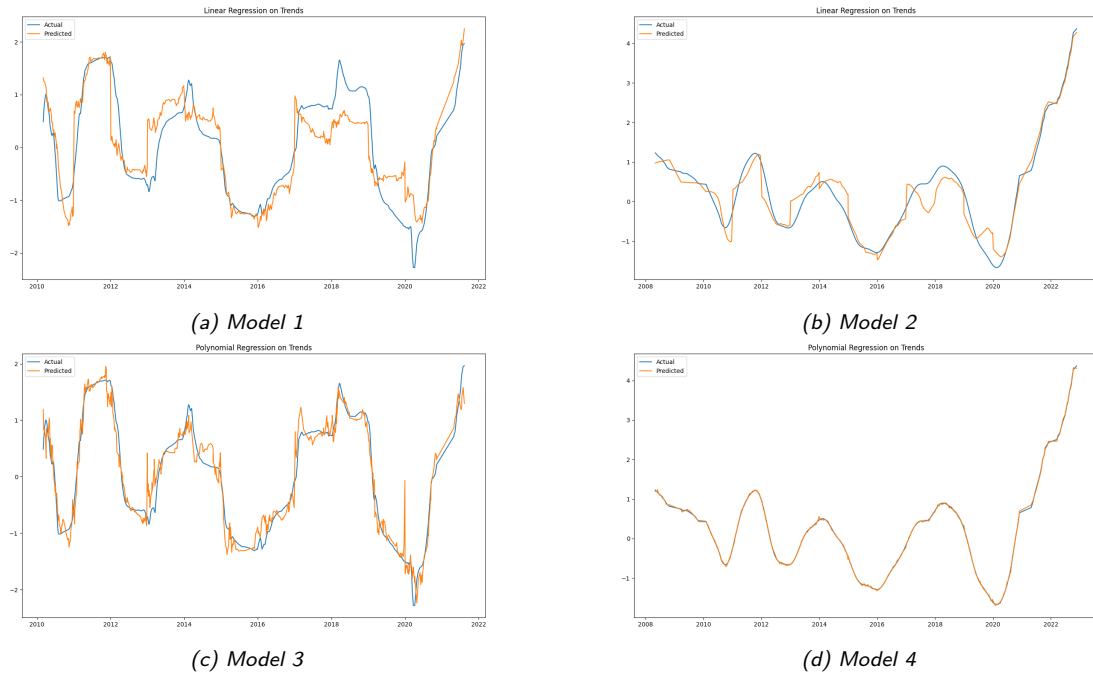


Figure 20: Linear regressions based on the four datasets prepared using TSD

The next step is recomposing the complete flowrate data by adding the extracted seasonal pattern to the projected trend. However, as an intermediary validation step, projected discharge trends are first added to the exact extracted seasonal pattern. The accuracy metrics for these four projections are recapitulated in Table 8. The results are coherent with the previous ones, showing that STL decomposition induces less significant MSE than classic TSD. The best MSE is 0.154, which does not demonstrate great accuracy but is still an improvement compared to the 0.239 and 0.579 values of, respectively, Random Forest and Linear Regression models without any flowrate feature.

No.	Model	Mean Squared Error
3	Model 4	0.15445
2	Model 3	0.16691
1	Model 2	0.21622
0	Model 1	0.23907

Table 8: Performance metrics of the superposition of projected trends with actual seasonal data

While the final step is still a work in progress, this approach has shown significant potential in answering the initial problem of making accurate long-term projections for Mekong River discharge in Stung Treng and, hence, for future hydropower generation in this location.

### 4.2.3 Additional studies

#### Description

First, nested cross-validation has been implemented to compare models without the bias of selecting them with the same dataset they are being evaluated with. The structure of this cross-validation is five outer loops and two inner loops. The models assessed through this method are Lasso, Ridge, and ElasticNet regressors, Quantile regressors (for low quantiles), and Decision Tree and Random Forest regressors. All models are available in the Scikit-learn library. Features are also added to the datasets, which are now the following:

- `data_mrc`: flowrate daily data for Stung Treng (1910-2024), Kratie (1924-2024), and Chiang Khan (1967-2024) (source: Mekong River Commission data portal)
- `data_mrc`: rainfall daily data for Stung Treng (2007-2024) and Chiang Khan (2008-2024) (source: Mekong River Commission data portal)
- `data_imf`: GDP annual data and forecasts for Thailand and Laos (1980-2029) (source: IMF)
- `temp_cambodia temp_month_cambodia`: Cambodia annual mean temperature (2007-2022) and monthly mean temperatures averaged by decade (1951-2020) (source: Climate change knowledge portal)
- `data_fao`: annual rice production in Cambodia and Laos (2005-2022) (source: Food and Agriculture Organization of the United Nations)
- `data_iea`: annual hydro and solar generation in Laos and Cambodia (2005-2021) (source: International Energy Agency).

Note that a "5-week total rainfall" feature, representing the sum of the daily rainfall for the past 5 weeks, is also added to the datasets. Training is done on data sorted by date instead of predicting using a shuffle. This ensures that models are suitable for actual data prediction.

Moreover, predictions are made for Stung Treng as before, but also for Chiang Khan (a Mekong station in Laos upstream from Vientiane) and for Kratie (in Cambodia, downstream from Stung Treng). The new models are recapitulated in the following list:

- Quantile regression for low flowrates on the Stung Treng and Chiang Khan datasets
- Nested cross-validation based on Stung Treng dataset
- Nested cross-validation based on the Chiang Khan dataset
- Models predicting Kratie flowrate based on Stung Treng's inputs
- Models predicting 2020-2021 flowrate based on Stung Treng dataset to study the impact of COVID-19 on river discharge and indirectly on water extraction
- Models trained on the Chiang Khan dataset and tested on the Stung Treng dataset
- Models trained on the Stung Treng dataset and tested on the Chiang Khan dataset.

## Results

After including the new features in the datasets, correlation heatmaps are computed to analyse feature interdependencies. The correlation matrices are below in Figure 21 and 22.

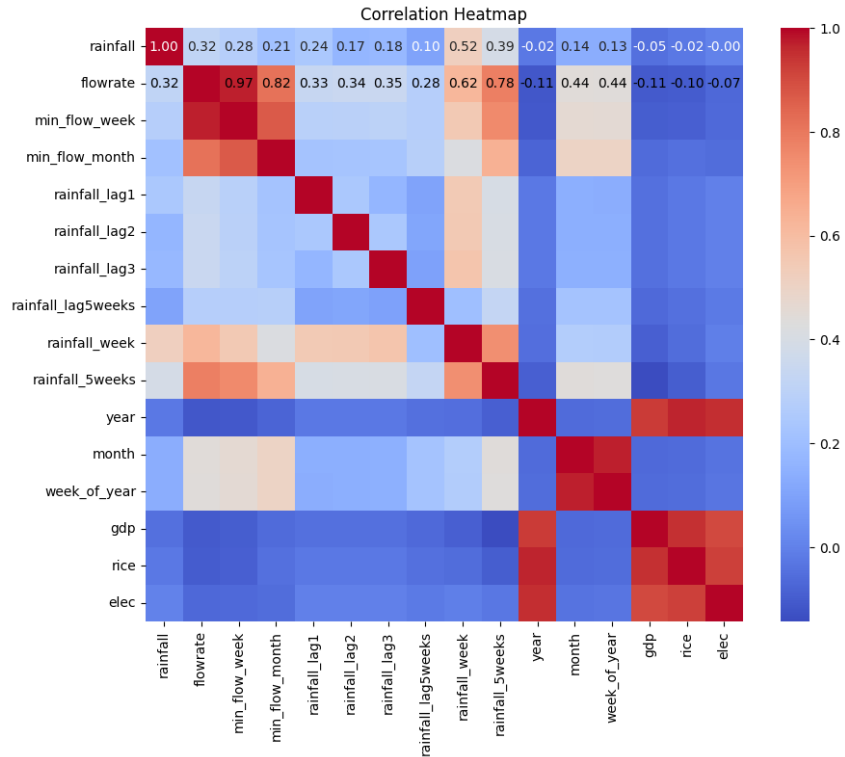


Figure 21: Stung Treng dataset correlation heatmap (elec = annual hydropower generation in Cambodia, rice = annual rice production in Cambodia, rainfall\_5weeks = total rainfall over the past 5 weeks)

For Figure 21, the most important features in relation to flowrate are the "baseline" flowrate (weekly or monthly), the rainfall over the last week, or even better, over the last five weeks, and a time index such as the month or the week of the year. Annual GDP, rice production and hydropower generation are closely correlated but have a lesser impact on flowrate. Thus, the features used to train and test the models are the following (for Chiang Khan, the same ".ck" features are used):

- daily rainfall: 'rainfall',
- year: 'year',
- month: 'month',
- week of the year: 'week\_of\_year',
- rainfall of the previous day: 'rainfall\_lag1',
- rainfall of day-2: 'rainfall\_lag2',
- rainfall of day-3: 'rainfall\_lag3',
- rainfall of week -5: 'rainfall\_lag5weeks',
- total rainfall over the past week: 'rainfall\_week',
- total rainfall over the past 5 weeks: 'rainfall\_5weeks',

- minimum flowrate of the previous month: 'min\_flow\_month',
- annual rice production of Cambodia: 'rice',
- annual hydropower generation of Cambodia: 'elec'

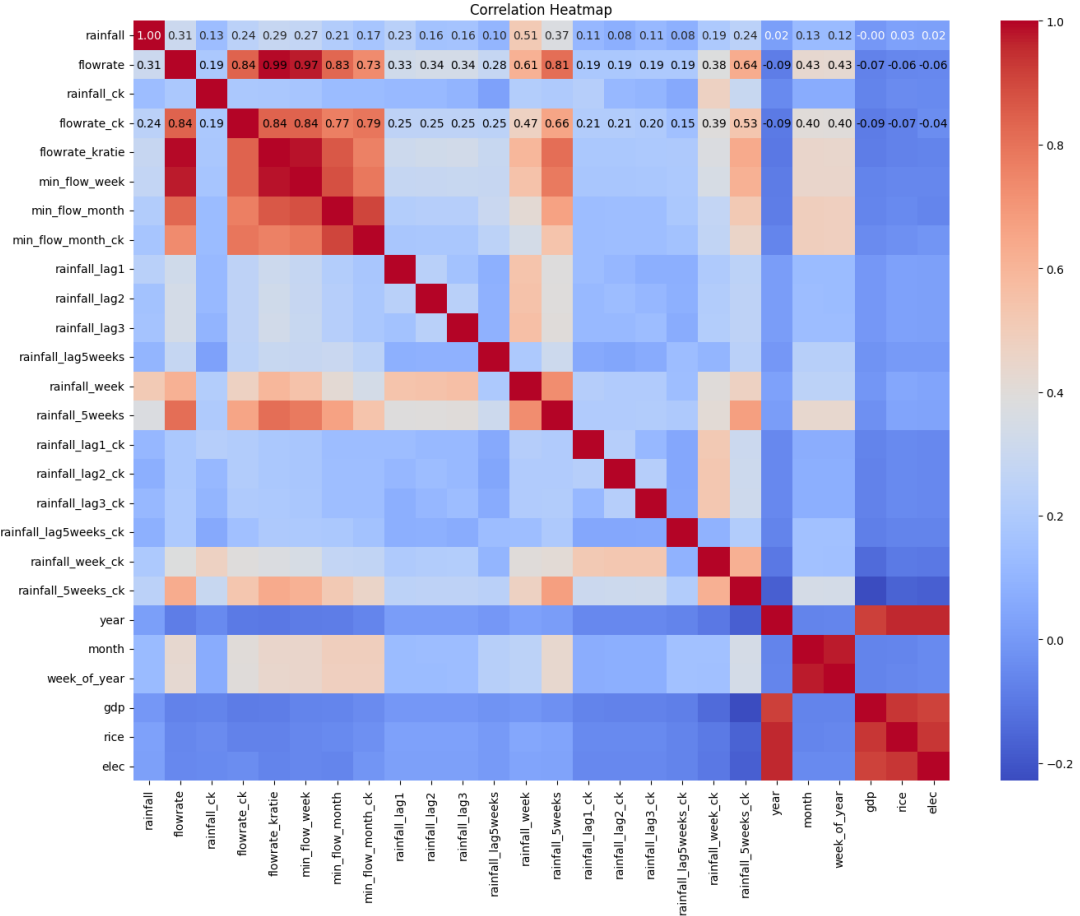


Figure 22: Chiang Khan and Stung Treng combined dataset correlation heatmap

First, the quantile regression models are implemented and evaluated on the test sets for both Chiang Khan and Stung Treng stations. The metrics obtained for these methods are recapitulated in Table 9 and the related plots are displayed in Figure 23.

Location	Test MSE	Test $R^2$
Stung Treng	0.2256	0.6715
Chiang Khan	0.2276	0.5605

Table 9: Quantile Regression ( $quantile=0.25$ ) Metrics for Stung Treng and Chiang Khan

On the plots, it can be noted that the models are indeed quite accurate for low flowrates, but a lot less for high flowrate, which is expected. However, finding an adequate threshold for the quantile used in the model is tricky because, for the 25th quantile used here, medium flowrates are not very accurate even though the global pattern of the data is reproduced by the models. Choosing a higher quantile, such as the 30th quantile, for instance, resulted in a decreased accuracy on low flowrates with unexpected small peaks

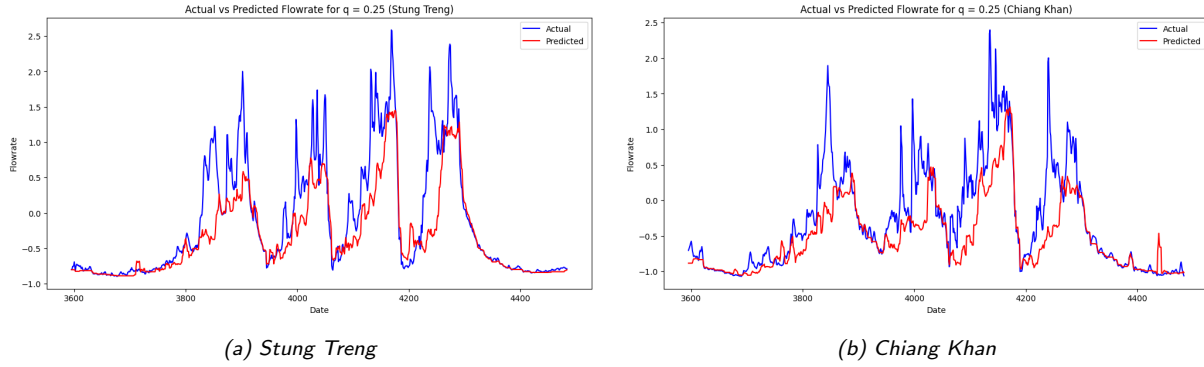


Figure 23: Plots of Stung Treng and Chiang Khan 25th quantile regressions

during dry-season weeks. Therefore, quantile regression can be a good solution to forecasts dry-season flowrates with a 25h quantile for instance, but another approach has to be designed to predict medium-to-high flowrates during the rest of the year.

Then, classic regressors predicting Stung Treng, Chiang Khan, and Kratie flow rates (based on Stung Treng climatic data in the last case) are compared using nested cross-validation, and the best-performing ones are evaluated on the test sets. The results are summed up in Table 10 and the plots are available in Figure ???. Indeed, the MSE and  $R^2$  score values are less relevant in this case than the models' ability to accurately capture the patterns of the actual data, which is why analysing the plots may be the best way to choose the best model.

Location	Model	Test MSE	Test $R^2$
Kratie	Lasso Regression	0.1953	0.6902
	Decision Tree Regression	0.3684	0.4157
	Random Forest Regression	0.2933	0.5349
Stung Treng	Lasso Regression	0.2317	0.6365
	Decision Tree Regression	1.0104	-0.5851
	Random Forest Regression	0.3566	0.4405
Chiang Khan	Lasso Regression	0.1669	0.3555
	Decision Tree Regression	0.6689	-1.5830
	Random Forest Regression	0.6099	-1.3553

Table 10: Evaluation Metrics for Kratie, Stung Treng, and Chiang Khan Forecasts

Thus, the Lasso regressor appears to be the best solution to our problem as it reproduces the data's patterns and intensity with great accuracy and is computationally efficient and fast. Random Forest is also efficient but less interpretable and more computationally intensive. Another perk of the Lasso regressor is that it combines L1-regularization and feature selection, as it can adjust the feature coefficients all the way to zero.

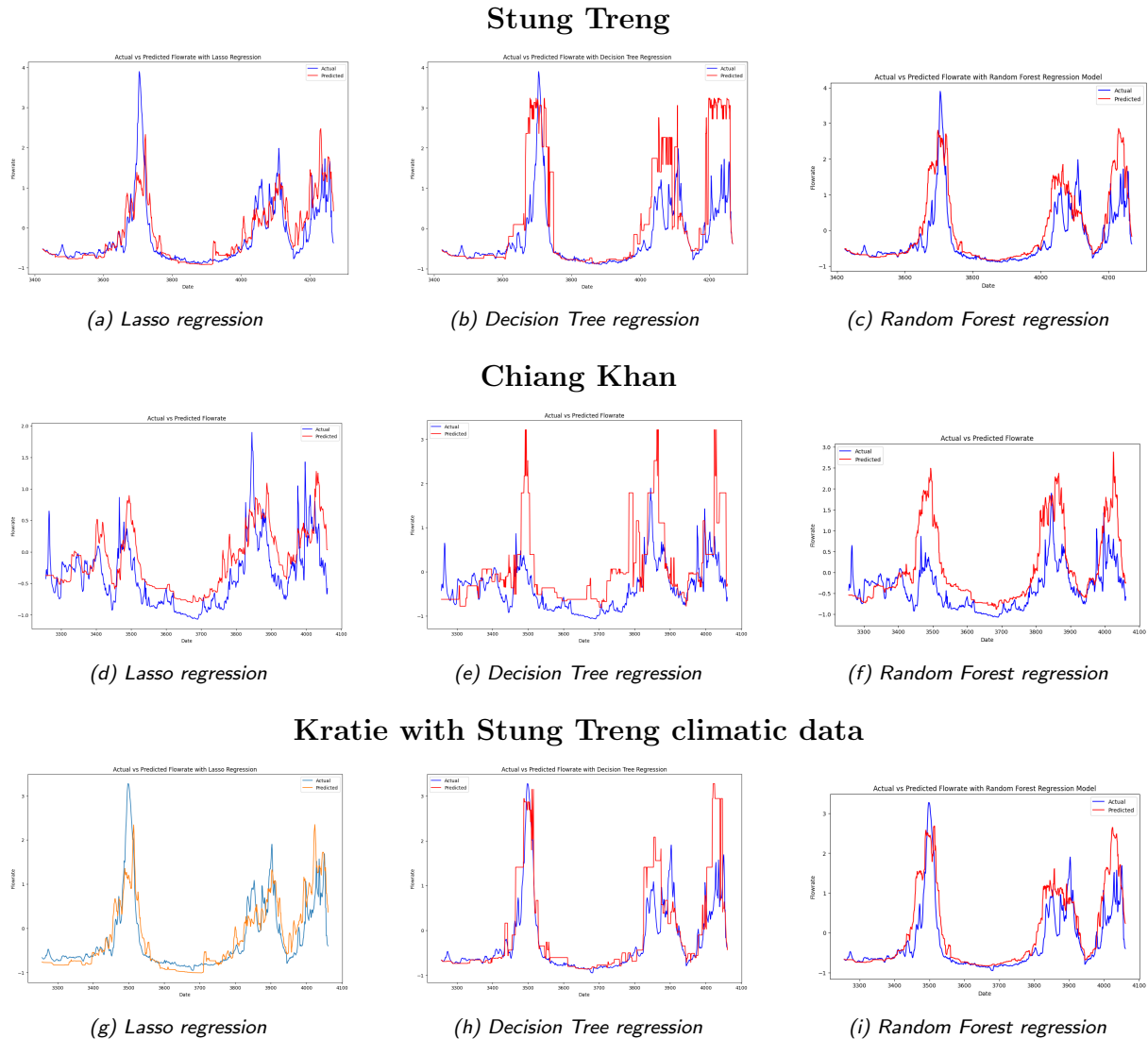


Figure 24: Regressors comparison for Stung Treng, Chiang Khan and Kratie

## 5 Code and datasets availability

The datasets and code files can be found in the GitHub repository using this link: <https://github.com/lelia-cv/Climate-change-SE-Asia-renewables>.

## **6 Conclusions**

This research, conducted as part of a comprehensive study on the impact of climate change on renewable power generation in Southeast Asia, specifically addresses the predictive accuracy of hydrological models for hydropower generation by focusing on the Stung Treng measurement station on the Mekong River. Through detailed statistical analysis and the application of interpretable machine learning models, the project sought to elucidate the complex interactions between climatic variables and river discharge, which are integral for improving hydropower forecasting and management.

While linear regression and decision tree regressors achieve acceptable accuracy, their performance diminishes when deprived of historical flowrate features. Although the potential relevance of incorporating human activity and water extraction indices has been acknowledged, this project has not explored these aspects in depth. A more thorough consideration of these elements could significantly enhance model accuracy and would be an exciting extension to this work. Additionally, implementing a hybrid projection model that combines regression projections from complete datasets with projections from monthly datasets for wet season months presents a promising avenue for future research.

Moreover, the findings demonstrate the utility of Time Series Decomposition (TSD) and Seasonal and Trend decomposition using Loess (STL) to identify underlying trends and seasonal patterns in hydrological data. The application of STL, in particular, shows promise in handling the non-linear and multifaceted nature of environmental data influenced by various climatic factors. However, the effectiveness of these methods varied, with STL decomposition providing more nuanced insights into the data's inherent patterns than classical TSD. While promising, this approach remains in development, and additional features such as water extraction, human activity, or climatic data could be added to the datasets to improve discharge projections. Experimenting with a Seasonal Autoregressive Integrated Moving Average (SARIMA) model also offers interesting perspectives.

Lastly, this work focuses exclusively on hydropower at a specific location, while the overarching research project aims to generalize these methods across a broader area in Southeast Asia while maintaining forecast accuracy for power generation. Consequently, this project still requires substantial effort, including expanding hydropower forecasting to encompass Southeast Asia and considering solar and wind power in future production forecasts. This field of research will undoubtedly demand rapidly increasing data and computational resources in the future, opening many perspectives for further studies.

## References

1. Liu, J., Chen, D., Mao, G., Irandehi, M. & Pokhrel, Y. Past and Future Changes in Climate and Water Resources in the Lancang–Mekong River Basin: Current Understanding and Future Research Directions. *Engineering* **13**. China, Sweden, USA, 144–152. ISSN: 20958099. <https://linkinghub.elsevier.com/retrieve/pii/S2095809921003593> (2024) (June 2022).
2. Wasti, A. *et al.* Climate change and the hydropower sector: A global review. *WIREs Climate Change* **13**. USA, UK, e757. ISSN: 1757-7780, 1757-7799. <https://wires.onlinelibrary.wiley.com/doi/10.1002/wcc.757> (2024) (Mar. 2022).
3. Intergovernmental Panel On Climate Change (Ipcc). *Climate Change 2021 – The Physical Science Basis: Working Group I Contribution to the Sixth Assessment Report of the Intergovernmental Panel on Climate Change* 1st ed. ISBN: 978-1-00-915789-6. <https://www.cambridge.org/core/product/identifier/9781009157896/type/book> (2024) (Cambridge University Press, July 6, 2023).
4. Turner, S. W., Ng, J. Y. & Galelli, S. Examining global electricity supply vulnerability to climate change using a high-fidelity hydropower dam model. *Science of The Total Environment* **590-591**, 663–675. ISSN: 00489697. <https://linkinghub.elsevier.com/retrieve/pii/S0048969717305272> (2024) (July 2017).
5. Wang, C. *et al.* Historical and projected future runoff over the Mekong River basin. *Earth System Dynamics* **15**, 75–90. ISSN: 2190-4987. <https://esd.copernicus.org/articles/15/75/2024/> (2024) (Jan. 29, 2024).
6. Li, D. *et al.* High Mountain Asia hydropower systems threatened by climate-driven landscape instability. *Nature Geoscience* **15**. China, Singapore, UK, Nepal, Australia, Kazakhstan, Netherlands, Switzerland, Canada, 520–530. ISSN: 1752-0894, 1752-0908. <https://www.nature.com/articles/s41561-022-00953-y> (2024) (July 2022).
7. Siala, K., Chowdhury, A. K., Dang, T. D. & Galelli, S. Solar energy and regional coordination as a feasible alternative to large hydropower in Southeast Asia. *Nature Communications* **12**. Singapore, USA, 4159. ISSN: 2041-1723. <https://www.nature.com/articles/s41467-021-24437-6> (2024) (July 6, 2021).
8. Russo, M., Carvalho, D., Martins, N. & Monteiro, A. Forecasting the inevitable: A review on the impacts of climate change on renewable energy resources. *Sustainable Energy Technologies and Assessments* **52**. Portugal, 102283. ISSN: 22131388. <https://linkinghub.elsevier.com/retrieve/pii/S2213138822003356> (2024) (Aug. 2022).
9. Mishra, S. K. *et al.* Differential Impact of Climate Change on the Hydropower Economics of Two River Basins in High Mountain Asia. *Frontiers in Environmental Science* **8**, 26. ISSN: 2296-665X. <https://www.frontiersin.org/article/10.3389/fenvs.2020.00026/full> (2024) (Mar. 13, 2020).
10. Grumbine, R. E., Dore, J. & Xu, J. Mekong hydropower: drivers of change and governance challenges. *Frontiers in Ecology and the Environment* **10**. China, USA, Australia, 91–98. ISSN: 1540-9295, 1540-9309. <https://esajournals.onlinelibrary.wiley.com/doi/10.1890/110146> (2024) (Mar. 2012).

11. Liu, L. *et al.* Climate change impacts on planned supply–demand match in global wind and solar energy systems. *Nature Energy* **8**. China, USA, Switzerland, UK, 870–880. ISSN: 2058-7546. <https://www.nature.com/articles/s41560-023-01304-w> (2024) (July 24, 2023).
12. Asian Development Bank. *Climate Change Operational Framework 2017-2030: Enhanced Actions for Low Greenhouse Gas Emissions and Climate-Resilient Development* Edition: 0 ISBN: 9789292579081 9789292579074 (Asian Development Bank, Manila, Philippines, Aug. 2017). <https://www.adb.org/documents/climate-change-operational-framework-2017-2030> (2024).
13. Thuy Hang, L. T., Sanseverino, E. R., Di Silvestre, M. L., Hai, P. M. & Ninh, N. Q. *Solar Power in Vietnam’s Energy Transition in 2023* Asia Meeting on Environment and Electrical Engineering (EEE-AM) 2023 Asia Meeting on Environment and Electrical Engineering (EEE-AM). Vietnam, Italy (IEEE, Hanoi, Vietnam, Nov. 13, 2023), 01–06. ISBN: 9798350381061. <https://ieeexplore.ieee.org/document/10394955/> (2024).
14. Sakti, A. D. *et al.* Spatial integration framework of solar, wind, and hydropower energy potential in Southeast Asia. *Scientific Reports* **13**. Indonesia, South Korea, Japan, Thailand, UK, Taiwan, 340. ISSN: 2045-2322. <https://www.nature.com/articles/s41598-022-25570-y> (2024) (Jan. 7, 2023).
15. Ibrahim, N. A., Wan Alwi, S. R., Abd Manan, Z., Mustaffa, A. A. & Kidam, K. Climate change impact on solar system in Malaysia: Techno-economic analysis. *Renewable and Sustainable Energy Reviews* **189**. Malaysia (2), 113901. ISSN: 13640321. <https://linkinghub.elsevier.com/retrieve/pii/S1364032123007591> (2024) (Jan. 2024).
16. Bhatt, U. S. *et al.* The Potential Impact of Climate Change on the Efficiency and Reliability of Solar, Hydro, and Wind Energy Sources. *Land* **11**. USA, Spain, 1275. ISSN: 2073-445X. <https://www.mdpi.com/2073-445X/11/8/1275> (2024) (Aug. 8, 2022).
17. Wu, R. *et al.* Future Projection and Uncertainty Analysis of Wind and Solar Energy in China Based on an Ensemble of CORDEX-EA-II Regional Climate Simulations. *Journal of Geophysical Research: Atmospheres* **129**. China (4), e2023JD040271. ISSN: 2169-897X, 2169-8996. <https://agupubs.onlinelibrary.wiley.com/doi/10.1029/2023JD040271> (2024) (Mar. 28, 2024).
18. Ismail, M. I., Yunus, N. A. & Hashim, H. The Challenges and Opportunities of Solar Thermal for Palm Oil Industry in Malaysia. *Chemical Engineering Transactions* **78**, 601–606. <https://www.cetjournal.it/> (2020).
19. Ibrahim Nur Atirah, Wan Alwi Sharifah Rafidah, Abdul Manan Zainuddin, Mustaffa Azizul Azri & Kidam Kamarizan. Impact of Drought Phenomenon on Renewable and Non-renewable Energy Systems in the ASEAN Countries. *Chemical Engineering Transactions* **83**. Malaysia, 73–78. <https://doi.org/10.3303/CET2183013> (2024) (Feb. 2021).
20. Gernaat, D. E. H. J. *et al.* Climate change impacts on renewable energy supply. *Nature Climate Change* **11**, 119–125. ISSN: 1758-678X, 1758-6798. <https://www.nature.com/articles/s41558-020-00949-9> (2024) (Feb. 2021).